



Contents lists available at ScienceDirect

## European Journal of Medicinal Chemistry

journal homepage: <http://www.elsevier.com/locate/ejmech>

## Discovery of novel BCR-ABL PROTACs based on the cereblon E3 ligase design, synthesis, and biological evaluation



Haixia Liu <sup>c, a, e, 1</sup>, Xinyu Ding <sup>a, b, e, 1</sup>, Linyi Liu <sup>d, 1</sup>, Qianglong Mi <sup>a, b</sup>, Quanju Zhao <sup>a</sup>, YuBao Shao <sup>f</sup>, Chaowei Ren <sup>a, b</sup>, Jinju Chen <sup>a</sup>, Ying Kong <sup>a</sup>, Xing Qiu <sup>g</sup>, Nicola Elvassore <sup>a</sup>, Xiaobao Yang <sup>a, \*</sup>, Qianqian Yin <sup>a, \*\*</sup>, Biao Jiang <sup>a, g, \*\*</sup>

<sup>a</sup> Shanghai Institute for Advanced Immunochemical Studies, China<sup>b</sup> School of Life Science and Technology, China<sup>c</sup> School of Physical Science and Technology, ShanghaiTech University, Shanghai, 201210, China<sup>d</sup> Hunan Provincial Key Laboratory of Tumor Microenvironment Responsive Drug Research, School of Pharmaceutical Science, University of South China, Hengyang City, 421001, China<sup>e</sup> University of Chinese Academy of Sciences, Beijing, 100049, China<sup>f</sup> Department of Histology and Embryology, Anhui Medical University, Hefei, 230032, China<sup>g</sup> CAS Key Laboratory of Synthetic Chemistry of Natural Substances, Shanghai Institute of Organic Chemistry, Chinese Academy of Sciences, 345 Lingling Road, Shanghai, 200032, China

## ARTICLE INFO

## Article history:

Received 2 April 2021

Received in revised form

9 June 2021

Accepted 9 June 2021

Available online 25 June 2021

## Keywords:

PROTAC

CRBN

Leukemia

BCR-ABL

Degradation

## ABSTRACT

Protein degradation is a promising strategy for drug development. Proteolysis-targeting chimeras (PROTACs) hijacking the E3 ligase cereblon (CRBN) exhibit enormous potential and universal degradation performance due to the small molecular weight of CRBN ligands. In this study, the CRBN-recruiting PROTACs were explored on the degradation of oncogenic fusion protein BCR-ABL, which drives the pathogenesis of chronic myeloid leukemia (CML). A series of novel PROTACs were synthesized by conjugating BCR-ABL inhibitor dasatinib to the CRBN ligand including pomalidomide and lenalidomide, and the extensive structure-activity relationship (SAR) studies were performed focusing on optimization of linker parameters. Therein, we uncovered that pomalidomide-based degrader **17** (SIAS056), possessing sulfur-substituted carbon chain linker, exhibits the most potent degradative activity *in vitro* and favorable pharmacokinetics *in vivo*. Besides, degrader **17** also degrades a variety of clinically relevant resistance-conferring mutations of BCR-ABL. Furthermore, degrader **17** induces significant tumor regression against K562 xenograft tumors. Our study indicates that **17** as an efficacious BCR-ABL degrader warrants intensive investigation for the future treatment of BCR-ABL<sup>+</sup> leukemia.

© 2021 Elsevier Masson SAS. All rights reserved.

## 1. Introduction

Proteolysis-targeting chimeras (PROTACs) have emerged as a potential strategy for drug discovery and design [1,2]. PROTACs, also known as degraders, are heterobifunctional molecules consisting of

a ligand targeting a protein of interest (POI), a ligand recruiting an E3 ligase and a connecting linker [3,4]. PROTACs are distinguished from classical inhibitors by inducing degradation of target proteins and not merely inhibition. A line of evidence uncover that PROTACs possess advantages over therapeutic inhibitors, including working at very low doses [5,6], overcoming potential resistance to current inhibitors [7,8], exerting improved selectivity [9,10] and having the potential to degrade undruggable targets [11,12]. PROTACs have exhibited remarkable biological activities in many target proteins [13,14] and ARV-110, a potential oral PROTAC targeting the androgen receptor, has shown benefit in patients with metastatic castration-resistant prostate cancer in early phase clinical trial [15].

Thalidomide, lenalidomide and pomalidomide are FDA approved drugs for the treatment of multiple myeloma termed the

\* Corresponding author. Shanghai Institute for Advanced Immunochemical Studies, ShanghaiTech University, Shanghai, 201210, China.

\*\* Corresponding author. Shanghai Institute for Advanced Immunochemical Studies, ShanghaiTech University, Shanghai, 201210, China.

\*\*\* Corresponding author. Shanghai Institute for Advanced Immunochemical Studies, ShanghaiTech University, Shanghai, 201210, China.

E-mail addresses: [xiaobaoyoung@126.com](mailto:xiaobaoyoung@126.com) (X. Yang), [yinqq@shanghaitech.edu.cn](mailto:yinqq@shanghaitech.edu.cn) (Q. Yin), [jiangbiao@shanghaitech.edu.cn](mailto:jiangbiao@shanghaitech.edu.cn) (B. Jiang).

<sup>1</sup> These authors contributed equally to this work.

immunomodulatory drugs (IMiDs) in clinic, target is the cereblon (CRBN) E3 ubiquitin ligase [16,17]. IMiDs have frequently been utilized as CRBN ligands for the design of PROTACs, possibly due to the relative safety and small molecular weight [18]. Furthermore, evidences showed that CRBN-recruiting PROTACs showed broader spectrum of protein degradation compared with VHL-based PROTACs [10,19].

The chimeric oncogenic fusion protein BCR-ABL is the key driving factor and therapeutic target of chronic myeloid leukemia (CML) [20,21]. The progression of BCR-ABL<sup>+</sup> CML can be effectively controlled with the clinical application of various BCR-ABL inhibitors such as imatinib, dasatinib and ponatinib [22]. However, several drawbacks including persistent leukemic stem cells retention and BCR-ABL kinase domain mutations as well as BCR-ABL kinase-independent signaling activation scream for new therapies [23–26]. Thus, exhaustive abrogation of BCR-ABL functions by PROTACs might have potential therapeutic benefits for CML treatment. In recent years, PROTACs targeting BCR-ABL have been uncovered to exhibit significant therapeutic potency [19,27–35]. Several PROTACs including **1** [19], **2** [30] and **3** [33] (Fig. 1), which recruit the CRBN E3 ligase, were identified to significantly degrade BCR-ABL at low nanomolar concentration. However, the structure-activity relationship (SAR), pharmacokinetic properties as well as the *in vivo* activity of CRBN-recruiting PROTACs targeting BCR-ABL have not been well investigated. To design novel BCR-ABL PROTACs hijacking CRBN and perform the SAR study, dasatinib was selected in our study as the BCR-ABL ligand for novel PROTACs design due to that dasatinib binds BCR-ABL both in its inactive and active conformation and exerted much greater potency compared with imatinib which binds BCR-ABL only in its inactive conformation, and shows efficacy against the majority of imatinib-resistant mutations (except the "gatekeeper" T315I) [36,37]. Herein, we described the design, synthesis, and evaluation of novel PROTACs targeting BCR-ABL by conjugating dasatinib to the CRBN ligands including pomalidomide and lenalidomide. A line of evidence in the field highlight the fact that linker composition and length play crucial roles in modulation of binding kinetics and the subsequent potency and selectivity [38–40]. Thus, a big challenge in PROTAC design is the selection of the optimal linker to connect these two binding ligands. In our previous work, we performed the SAR study of VHL-recruiting PROTACs targeting BCR-ABL based on dasatinib and identified **SIAIS178**, possessing a carbon chain linker, was the most potent one among the VHL-based PROTACs by inducing more robust ternary complex formation [28]. On this basis, the extensive optimization of linker parameters such as length, hydrophilicity and rigidity was investigated in our study. We uncovered that pomalidomide-based degrader **17** (**SIAIS056**), possessing sulfur-

substituted carbon chain linker, achieves the most potent BCR-ABL-degrading activity *in vitro*. Additionally, degrader **17** also induces the degradation of several clinically relevant resistance-conferring mutations of BCR-ABL. Moreover, degrader **17** exerts favorable pharmacokinetics and induces substantial tumor regression against K562 xenograft tumors *in vivo*. Collectively, our study provided a deeper understanding for the development of BCR-ABL PROTACs and novel potential therapeutic agents for CML treatment.

## 2. Results and discussion

### 2.1. Chemistry

The general reactions utilized for synthesis of the novel targeted derivatives are outlined in Schemes 1–6. All the starting materials were commercially available. First, the precursor of ABL inhibitor dasatinib **S2** was obtained from **S1** by substitution reaction. As shown in Scheme 1, the furnished 4-F-thalidomide **S3** subsequently reacted with various amines by nucleophilic substitution following cleavage to form intermediates **S5** or **S7**. Then derivatives **4–11**, **13** were obtained through condensation of **S2** with corresponding **S5** or **S7**. Then thiolation and etherification of **S3** produced the intermediate **S9**, which was converted to **S10** by removal of *tert*-butyl group. After condensation of **S2**, **S10** was transformed into derivative **12** (Scheme 2). Meanwhile, **S9** was oxidized to afford **S11**, which was followed by removal of *tert*-butyl group to get intermediate **S12**. After condensation with **S2**, **S12** was converted into derivative **16** (Scheme 2).

As shown in Scheme 3, following condensation and etherification, **S13** was translated into **S15** which was hydrolyzed following condensation to get derivative **14**. Further, after condensation and palladium-catalyzed cross coupling reaction as well as hydrogenation and hydrolysis, the intermediate **S20** was obtained from **S17** through reacting with corresponding reagents. Afterwards, derivative **15** was obtained through the condensation of **S20** with **S2** (Scheme 3). The intermediate **S23** derived from **S21** was etherified with thiolated pomalidomide derivatives **S8** or **S8-1** as well as lenalidomide derivative **S24** to afford corresponding **17**, **24** or **19**, respectively (Scheme 4). Following thiolation reaction and the subsequent sulfide formation and the cleavage of *tert*-butyl esters, lenalidomide was transformed into **S27**, which condensed with **S2** to obtain derivative **18** as depicted in Scheme 4.

Finally, **S2** reacted with *tert*-butyl (4-bromobutyl) carbamate to produce **S28**. After deprotection, the product reacted with **S3** to afford **20**. Hereafter, derivative **21** was obtained from pomalidomide **S29** following acylation reaction and electrophilic

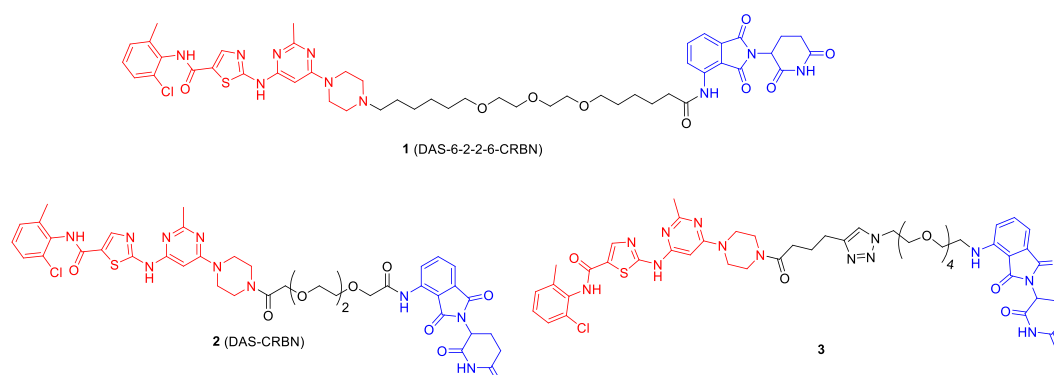
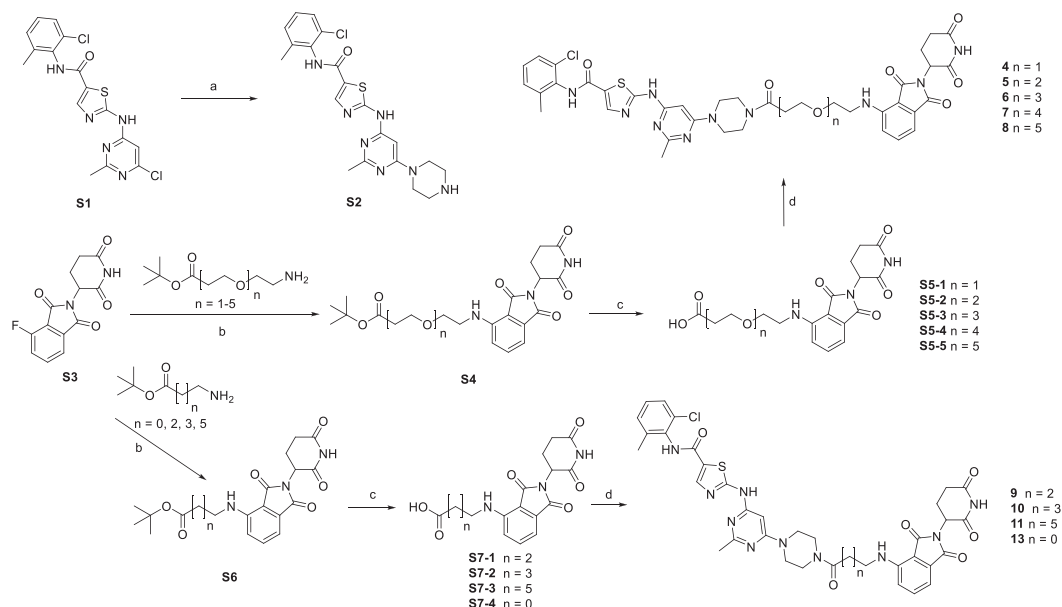
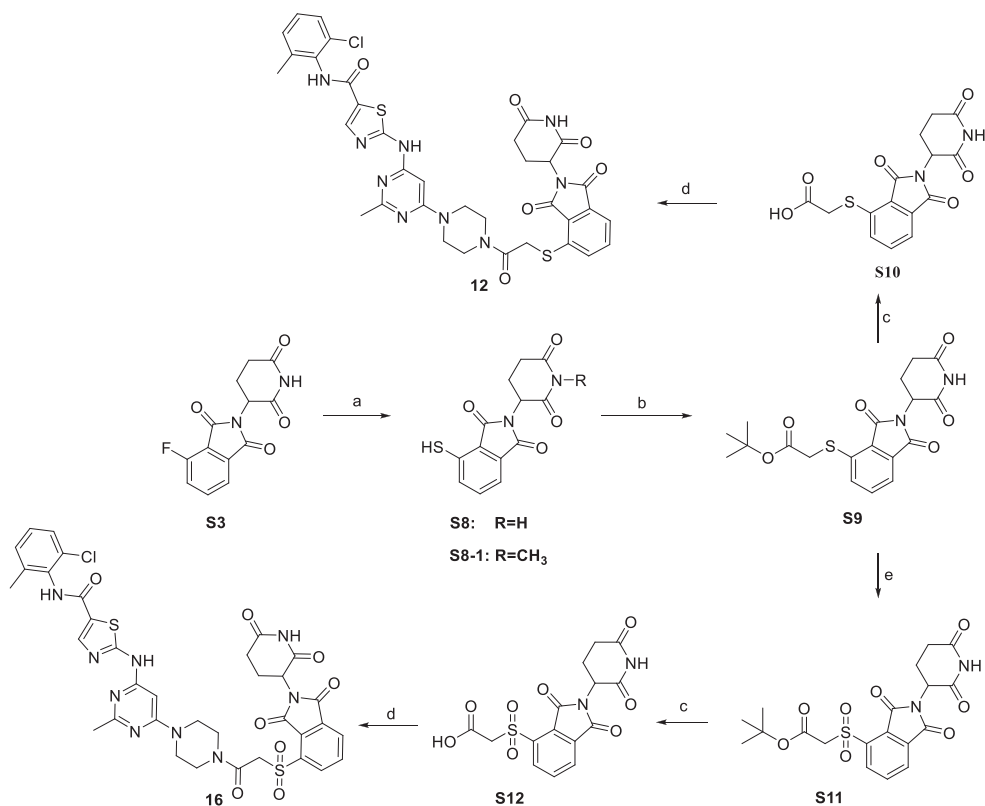


Fig. 1. Reported effective BCR-ABL PROTACs based on CRBN.



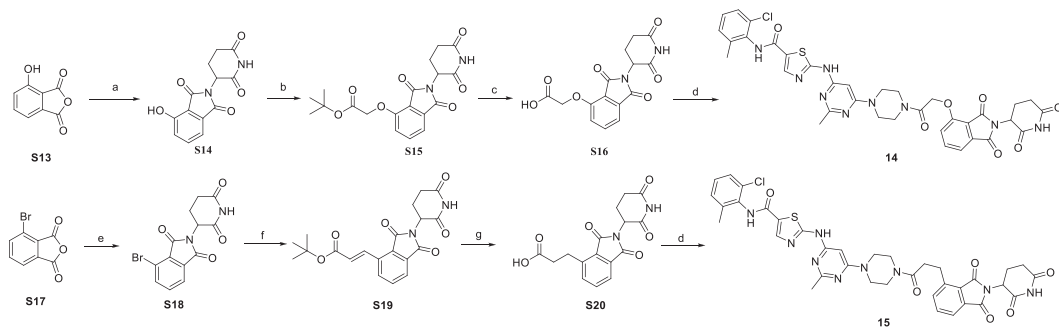
**Scheme 1.** Reagents and conditions: a) piperazine, DIPEA, *n*-BuOH, 110 °C, 16 h; b) DIPEA, NMP, 110 °C, MW, 2 h; c) 88% HCOOH, 25 °C, 12 h; d) **S2**, HOAt, EDCI, NMM, DMF, 25 °C, 12 h.



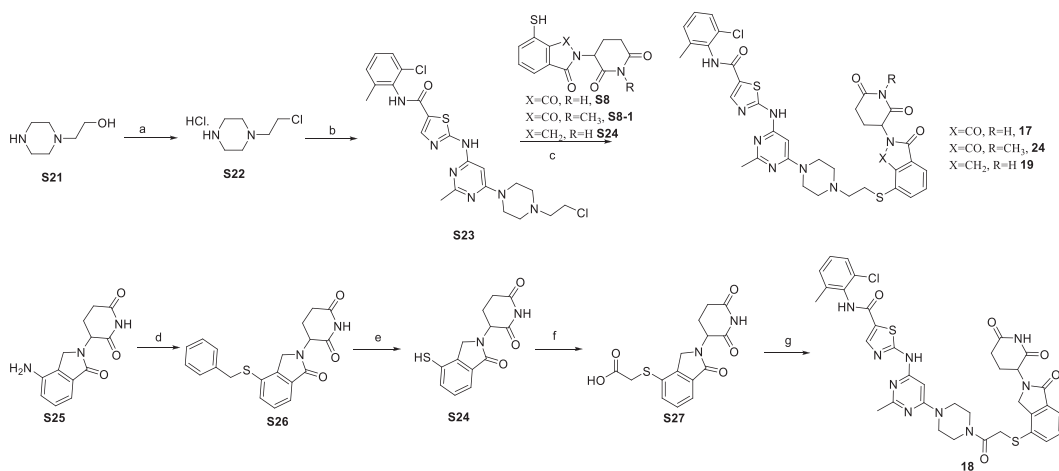
**Scheme 2.** Reagents and conditions: a) **S8**: Na<sub>2</sub>S<sub>9</sub>H<sub>2</sub>O, DMF, 25 °C, 0.5 h; **S8-1**: i, K<sub>2</sub>CO<sub>3</sub>, NaI, CH<sub>3</sub>I, rt, 0.5 h; ii, Na<sub>2</sub>S<sub>9</sub>H<sub>2</sub>O, DMF, N<sub>2</sub>, 25 °C, 3 h; b) *tert*-butyl 2-bromoacetate, K<sub>2</sub>CO<sub>3</sub>, DMF, 25 °C, 0.5 h; c) 88% HCOOH, 25 °C, 12 h; d) **S2**, HOAt, EDCI, NMM, DMF, 25 °C, 12 h; e) *m*-CPBA, DCM, 40 °C, 4 h.

substitution (Scheme 5). The syntheses of derivatives **22**, **23** were performed as depicted in Scheme 6. On one hand, lenalidomide **S31** afforded the intermediate **S32** following substitution and the cleavage of *tert*-butyl esters. After that, **S32** condensed with **S2** to yield compound **22**. On the other hand, derivative **23** was yielded

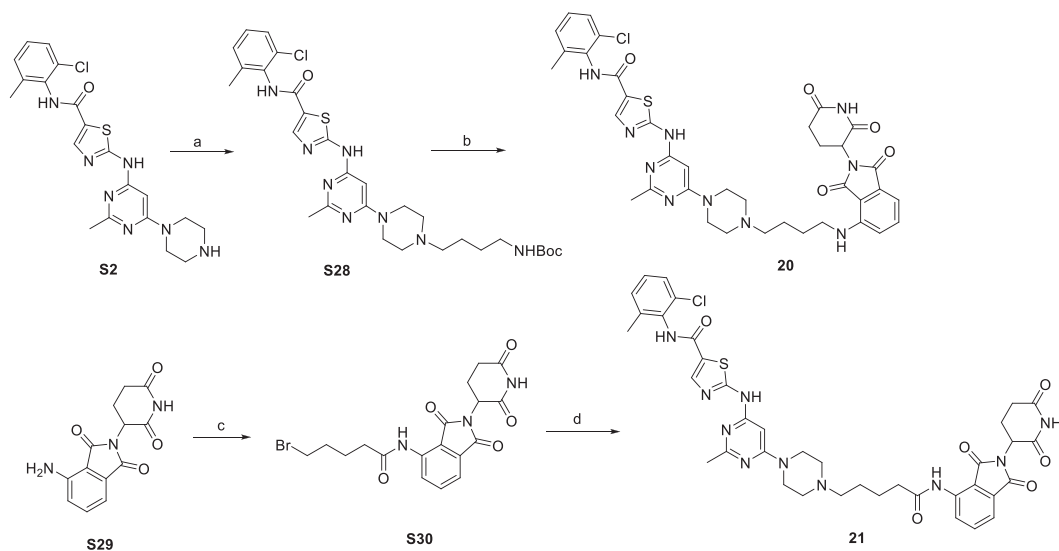
through two condensation reactions from starting material **S31**. All the synthesized compounds have been confirmed by NMR and mass spectrometry.



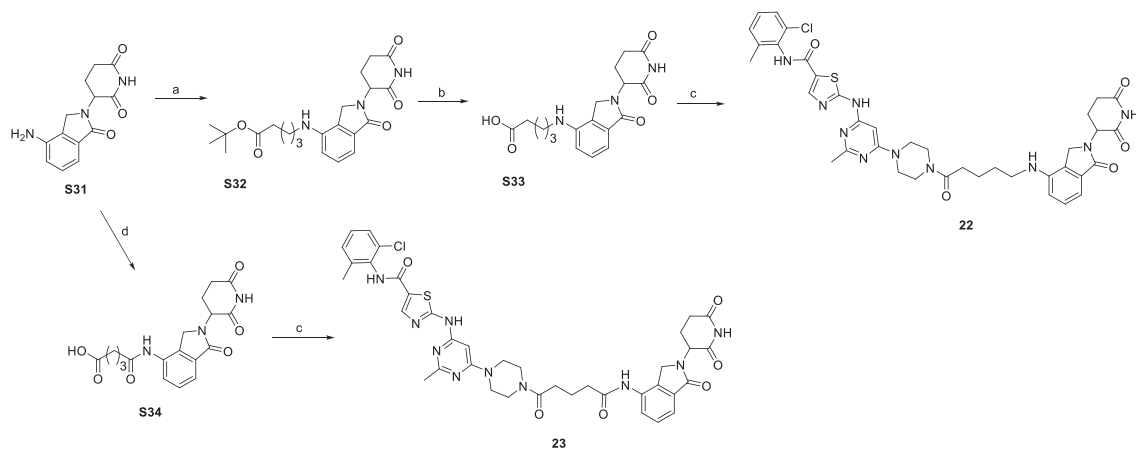
**Scheme 3.** Reagents and conditions: a) 3-aminopiperidine-2,6-dione, TEA, Toluene, reflux, 12 h; b) *tert*-butyl 2-bromoacetate, NaHCO<sub>3</sub>, KI, DMF, 60 °C, 12 h; c) TFA, DCM, rt, 2 h; d) **S2**, HOAt, EDCI, NMM, DMF, 25 °C, 12 h; e) 3-aminopiperidine-2,6-dione, NaOAc, AcOH, reflux, 12 h; f) *tert*-butyl acrylate, Pd<sub>2</sub>(dba)<sub>3</sub>, Cy<sub>2</sub>NME, HP(*t*-Bu)BF<sub>4</sub>, Dioxane, 55 °C, 12 h; g) 10% Pd/C, Dioxane, rt, 12 h; ii: TFA, DCM, rt, 2 h.



**Scheme 4.** Reagents and conditions: a) sulfurous dichloride, Reflux, 12 h; b) DIPEA, DMF, 110 °C, 12 h; c) NaI, K<sub>2</sub>CO<sub>3</sub>, DMF, 60 °C, 8 h; d) BnCl, Na<sub>2</sub>S<sub>2</sub>O<sub>3</sub>·5H<sub>2</sub>O, CuSO<sub>4</sub>·5H<sub>2</sub>O, Biby, *t*-BuONO MeOH, H<sub>2</sub>O, 80 °C, 8 h; e) AlCl<sub>3</sub>, Toluene, 35 °C, 12 h; f) *tert*-butyl 2-bromoacetate, K<sub>2</sub>CO<sub>3</sub>, DMF, 25 °C, 2 h; ii: 88% HCOOH, 25 °C, 12 h; g) **S2**, HOAt, EDCI, NMM, DMF, 25 °C, 12 h.



**Scheme 5.** Reagents and conditions: a) *tert*-butyl (4-bromobutyl)carbamate, K<sub>2</sub>CO<sub>3</sub>, NaI, DMF, 110 °C, 12 h; b) i: HCOOH, rt, 12 h; ii: **S3**, DIPEA, NMP, 110 °C, 4 h; c) 5-bromopentanoyl chloride, THF, reflux, 3 h; d) **S2**, NaI, K<sub>2</sub>CO<sub>3</sub>, DMF, 60 °C, 4 h.



**Scheme 6.** Reagents and conditions: a) *tert*-butyl 5-bromopentanoate, DIPEA, NMP, 100 °C, 12 h; b) TFA, DCM, rt, 1 h; c) **S2**, HOAt, EDCI, NMM, DMF, 25 °C, 12 h; d) glutaric acid, HOAt, EDCI, NMM, DCM/DMF, 0 °C–25 °C, 12 h.

## 2.2. Biological evaluation

### 2.2.1. Anti-proliferative activities and BCR-ABL-degrading activity

All synthesized compounds were evaluated for their anti-proliferative activity on BCR-ABL driven CML cell line K562 cells and degradative activity against BCR-ABL. For comparison, CRBN ligands (pomalidomide and lenalidomide) and BCR-ABL inhibitor dasatinib as well as reported CRBN-based PROTAC DAS-6-2-2-6-CRBN (**1**) were also included as reference compounds. As shown in Table 1, these initially synthesized compounds effectively

inhibited K562 cell proliferation with the growth inhibitory potency ( $IC_{50}$ ) value at low nanomolar concentration except for CRBN ligands pomalidomide (poma) and lenalidomide (lena). Moreover, compound **10** exhibited similar anti-proliferative activities to dasatinib (Das). Furthermore, all these PROTACs induced BCR-ABL degradation with the degradation potency ( $DC_{50}$ ) value at low nanomolar concentrations. However, the ligands of BCR-ABL (Das) and E3 ligase (poma and lena) didn't decrease the BCR-ABL protein level even at 10  $\mu$ M concentration. Among them, compounds **4**, **9** and **11** were about 3 times more active than compound **1** in BCR-

**Table 1**  
The anti-proliferative activities against K562 and BCR-ABL-degrading activity of derivatives **4–11** with PEG- or Carbon-based linkers.

Compound	Linker	X	K562 $IC_{50}$ (nM)	BCR-ABL $DC_{50}$ (nM)
Pomalidomide	—	—	>10 $\mu$ M	>10 $\mu$ M
Lenalidomide	—	—	>10 $\mu$ M	>10 $\mu$ M
Dasatinib	—	—	0.9	>10 $\mu$ M
<b>1</b> (DAS-6-2-2-6-CRBN)	—	CO	4.1	30.5
<b>4</b>		CO	18.42	8.7
<b>5</b>		CO	8.05	17.5
<b>6</b>		CO	14.75	18.4
<b>7</b>		CO	40.4	26.1
<b>8</b>		CO	31.9	10.8
<b>9</b>		CO	5.5	7.8
<b>10</b>		CO	0.55	11
<b>11</b>		CO	1.47	9

ABL degradation. Interestingly, some compounds (**4–9**), possessing better degradation potency, showed attenuated anti-proliferative activities compared to **1**, that is, the DC<sub>50</sub> and IC<sub>50</sub> are not parallel. We speculated that the unparalleled DC<sub>50</sub> and IC<sub>50</sub> are possibly due to that PROTAC-induced growth inhibition is a consequence of the dual action of both inhibition and degradation of BCR-ABL proteins, and there seems to be no good correlation between the two capacities of PROTACs, just as the results reported by Crews [19], in which PROTACs exerting significant ABL inhibition (non-phosphorylated or phosphorylated) didn't substantially degrade BCR-ABL. Collectively, the results clarified that carbon-based linkers can cause similar degradation efficacy to PEG-based linkers. Meanwhile, these PROTACs composed of linkers of different lengths all induced significant degradation of BCR-ABL, indicating that the length of linkers seems not to be the key factor in BCR-ABL degradation for CRBN-based PROTACs.

Hereafter, several derivatives which contain linkers of three atoms length with varying heteroatoms (S, N, O) and carbon atom connected to C-4 position of pomalidomide were synthesized and investigated. As depicted in Table 2, all compounds exhibited significant anti-proliferative activities and BCR-ABL-degrading activities in K562 cells. In detail, the sulfur-substituted compound **12** exhibited the best degradative activity with DC<sub>50</sub> value about 5.6 nM. When sulfur atom is substituted by NH (compound **13**) or O (compound **14**), there was a slight decrease in the DC<sub>50</sub> (about 10 nM). Substitution of S atom with C atom, the BCR-ABL-degrading activity of the generated **15** is 17 times less potent than that of **12**. Inversion S atom in **12** with sulphone, the generated compound **16** was about 50 times less potent than **12** in BCR-ABL degradation. Moreover, the anti-proliferative activity of **16** also significantly decreased accompanied with reduction of degradation potency of BCR-ABL. All these results suggested that the groups substituted at C-4 of pomalidomide influence the BCR-ABL-degrading activity and derivatives with substitution of S atom are more potent in BCR-ABL degradation than those with substitution of other atoms.

Meanwhile, a series of acyl-substituted derivatives were synthesized to explore the influence of the acyl group on biological activities. As shown in Table 3, we found that the acyl substitution at piperazine of dasatinib was adverse to the BCR-ABL-degrading activity (**12** vs **17**, **18** vs **19**, respectively). Compounds **17** and **19**, in which dasatinib was conjugated by alkylation substitution

**Table 2**  
The anti-proliferative activities against K562 and BCR-ABL-degrading activity of derivatives **12–16** having linkers with different atoms connected to C-4 of pomalidomide.

Compound	Linker	X	K562 IC <sub>50</sub> (nM)	BCR-ABL DC <sub>50</sub> (nM)
<b>12</b>		CO	3.2	5.6
<b>13</b>		CO	1.22	10
<b>14</b>		CO	7	11.1
<b>15</b>		CO	2.84	95.4
<b>16</b>		CO	206	245.1

**Table 3**  
The anti-proliferative activities against K562 and BCR-ABL-degrading activity of derivatives **17–23** with or without acyl substitution.

Compound	Linker	X	K562 IC <sub>50</sub> (nM)	BCR-ABL DC <sub>50</sub> (nM)
<b>17</b> (SIAIS056)		CO	0.49	0.18
<b>18</b>		CH <sub>2</sub>	5.7	8.9
<b>19</b>		CH <sub>2</sub>	0.51	2.7
<b>20</b>		CO	0.28	2.7
<b>21</b>		CO	4.6	10.1
<b>22</b>		CH <sub>2</sub>	4.2	11.1
<b>23</b>		CH <sub>2</sub>	1.03	125

exhibited more potent BCR-ABL-degrading activity with DC<sub>50</sub> value of 0.18 nM and 2.7 nM, respectively. Notably, **17** based on pomalidomide possesses more potent degradative activity than **19** based on lenalidomide. Furthermore, with insertion of carbonyl group at amine group of pomalidomide or lenalidomide, the BCR-ABL-degrading activity also decreased (**20** vs **21**, **22** vs **23**, respectively). In brief, PROTACs containing the alkylated linkers are more potent in BCR-ABL degradation than those having linkers with the acyl substitution group, while the acyl substitution on the end of linkers was harmful to the BCR-ABL-degrading activity.

Herein, we summarized the SAR study according to the results above (Fig. 2). First, the length of linkers based on either PEG-containing (-O-CH<sub>2</sub>-CH<sub>2</sub>-O-) linkers or carbon-containing linkers seem not to be an important factor in BCR-ABL degradation and this will help us find potent PROTACs with smaller molecular weight. Secondly, alkylated conjunction of dasatinib and CRBN ligands (pomalidomide and lenalidomide) exerts the better activity than acetylated conjunction between these two ligands in BCR-ABL

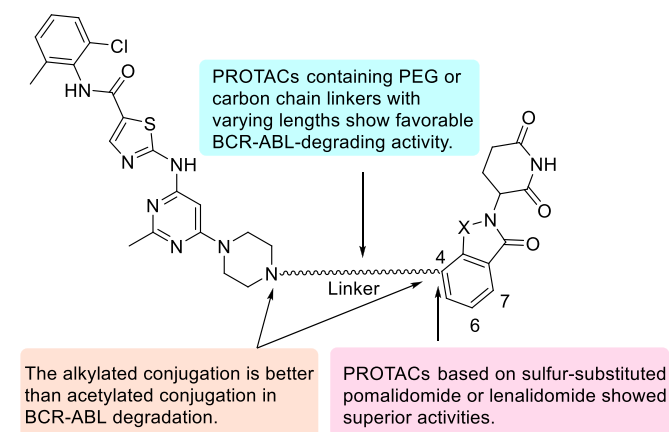


Fig. 2. A summary of SAR on BCR-ABL degradation.

degradation. Moreover, the substitutions of heteroatoms and carbon atom at C-4 position of pomalidomide or lenalidomide provoke different degradative ability and PROTACs based on sulfur-substituted pomalidomide showed superior proliferative inhibitory and BCR-ABL-degrading activities.

### 2.2.2. The linkers' influence on PK properties of PROTACs

On the basis of chemical structure and biological evaluation above, PROTACs including **5**, **17** and **20** were further performed to evaluate their pharmacokinetics (PK) properties. These compounds were administered intravenously to the femoral vein of female Wistar rats at 2 mg/kg. The results were shown in Table 4. Compound **17** was shown to have superior pharmacokinetic profiles relative to others in half-life ( $T_{1/2}$ ), and both of **17** and **20** displayed lower clearance rate than **5**. On the contrary, compound **5** exhibited poor pharmacokinetic profiles. Unfortunately, the oral bioavailability of all these compounds is unsatisfactory (data not shown). Conclusively, the PK result indicated that the linkers of different lengths and compositions could influence the PK properties of PROTACs *in vivo*. Compound **17**, containing the sulfur-substituted linkers, resulted in a dramatically improved pharmacokinetic profiles *in vivo*, with a prolonged  $T_{1/2}$ , increased plasma concentration, and increased area under the plasma concentration-time curve (AUC), and will be utilized for further *in vivo* studies. The superior pharmacokinetic profiles of compound **17** may be due to that its linker parameters such as length, hydrophilicity and rigidity possibly improved stability or cell membrane permeability *in vivo*. Further ADME studies may be needed to be explored in the future.

### 2.2.3. Degradation of BCR-ABL induced by **17** in dose and time dependent manner

To confirm the mechanistic involvement of CRBN E3 ubiquitin ligase for BCR-ABL degrading activity of compound **17** (**SIAIS056**), we prepared inactive compound **24** (Fig. 3) which contained a methyl group at N of glutarimide as a negative control. The inactive compound **24** showed reduced anti-proliferative activity against K562 cells and 32D cells exogenously expressing wide-type BCR-ABL compared with **17** (Supporting Fig. S1). Moreover, the degrader **17** dramatically decreased the protein level of BCR-ABL and c-ABL at dose dependent manner (Fig. 4A), while dasatinib and **24** failed to induce BCR-ABL and c-ABL degradation (Fig. 4A and B). Meanwhile, the BCR-ABL signaling activity, indicated as the phosphorylation of BCR-ABL and its downstream proteins including STAT5 (signal transducer and activator of transcription 5) and CRKL (Crk like proto-oncogene), were significantly inhibited by both **17** and **24** (Fig. 4A and B). Of note, degrader **17** also induced the degradation of Src, but not PDGFR $\beta$  (Supporting Fig. S2), which are the potential targets of dasatinib [36], indicating that the selectivity of PROTACs was improved over parent inhibitor. Furthermore, the time-course

results showed that dramatic reduction of BCR-ABL was observed after 4 h treatment of **17** at the 30 nM concentration (Fig. 4C). Consistently, **17** also time-dependently inhibited the BCR-ABL signaling, accompanied with decreased phosphorylation of BCR-ABL and its downstream molecules STAT5 and CRKL. Additionally, the time-course effects of **17** on turnover of BCR-ABL protein was also assessed by adding a protein synthesis inhibitor cycloheximide (CHX). The accelerated turnover rate of BCR-ABL and c-ABL proteins were observed following treatment of **17** as compared to that of vehicle treatment, further supporting the BCR-ABL-degrading efficacy of **17** in K562 cells (Supporting Fig. S3A and Fig. S3B). Moreover, the pretreatment of pomalidomide or dasatinib, and proteasome inhibitor MG132 as well as NEDD8-activating enzyme (NAE) inhibitor MLN4924 significantly blocked the degrader **17**-induced degradation of BCR-ABL and c-ABL in a competition assay (Fig. 4D), suggesting that **17**-induced target protein degradation is dependent on the CRBN ubiquitin ligase and consistent with the nature of PROTAC principle.

As we mentioned in the introduction, this work builds on our own previous work [28], in which the SAR study of VHL-recruiting PROTACs targeting BCR-ABL was conducted and the most potent degrader **SIAIS178** was identified to induce effective degradation of BCR-ABL protein. The comparison between **17** and **SIAIS178**, the two most active BCR-ABL PROTACs of our CRBN- and VHL-recruiting BCR-ABL PROTAC series respectively, is worthy of further discussion. First, both of **17** and **SIAIS178** possessed carbon alkyl chain  $-(CH_2)_n-$  linkers conjugating dasatinib to the corresponding E3 ligands, which suggested that the alkylated chain linker could be considered for the future design of novel PROTACs to achieve effective BCR-ABL degradation. Secondly, the degrader **17** showed more potent *in vitro* anti-proliferative and BCR-ABL-degrading activity than **SIAIS178**, further indicating that CRBN-recruiting PROTACs exhibit more effective and broader spectrum of protein degradation compared with VHL-based PROTACs, which was in line with previous literatures [10,19]. Additionally, the degrader **17**, which presented smaller molecular weight and shorter chain length than **SIAIS178**, to some extent, may have more potential for the CML therapy and be worthy of further study.

### 2.2.4. Degradation of BCR-ABL mutations induced by **17**

Degrader **17** was further investigated to evaluate the potential ability to overcome resistance to currently clinical tyrosine kinase inhibitors treatment primarily associated with the BCR-ABL mutations. Herein, murine myeloid cell line 32D was transduced with retroviral vector carrying wide-type BCR-ABL as well as various clinically relevant BCR-ABL mutant isoforms and the degradation was further evaluated by western blotting. Among them, G250E, E255K, F317L and T315I were imatinib-resistant mutants. E255K, V299L, F317V, F317L, T315A and T315I were associated with

**Table 4**  
The PK assay of compound **5**, **17** and **20** in rat (*iv*).

Compound	$T_{1/2}$ <sup>a</sup> h	$T_{max}$ <sup>b</sup> h	$C_{max}$ <sup>c</sup> ng/mL	$AUC_{(0-t)}$ <sup>d</sup> h*ng/mL	$MRT_{(0-t)}$ h	$V_{ss}$ <sup>e</sup> mL/kg	$V_z$ <sup>f</sup> mL/kg	Cl <sup>g</sup> mL/h/kg
<b>5</b>	0.62	0.08	1142.78	496.43	0.45	1929.82	3591.00	4026.80
<b>17</b> (SIAIS056)	4.23	0.08	1497.45	926.29	2.00	5225.18	13046.83	2140.26
<b>20</b>	1.93	0.08	1449.44	1331.45	1.55	2783.19	4020.74	1448.68

Abbreviations: AUC, area under the plasma concentration-time curve; MRT, mean residence time.

<sup>a</sup>  $T_{1/2}$ , elimination half-life.

<sup>b</sup>  $T_{max}$ , time taken to reach peak plasma concentration.

<sup>c</sup>  $C_{max}$ , maximum (peak) plasma drug concentration.

<sup>d</sup>  $AUC_{(0-t)}$ , AUC from time zero to time t.

<sup>e</sup>  $V_{ss}$ , the apparent volume of distribution during steady state.

<sup>f</sup>  $V_z$ , apparent volume of distribution during the terminal phase.

<sup>g</sup> Cl, apparent total body clearance of the drug from plasma.

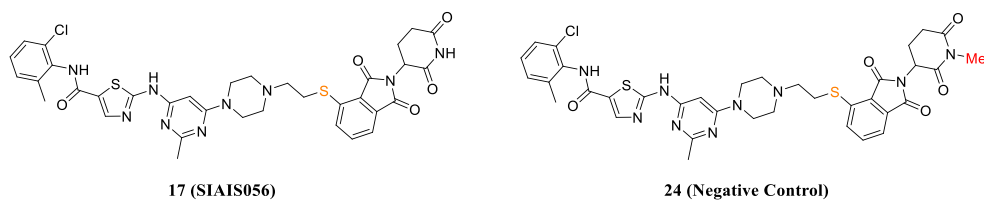


Fig. 3. The structure of compound **17** and its negative control **24**.

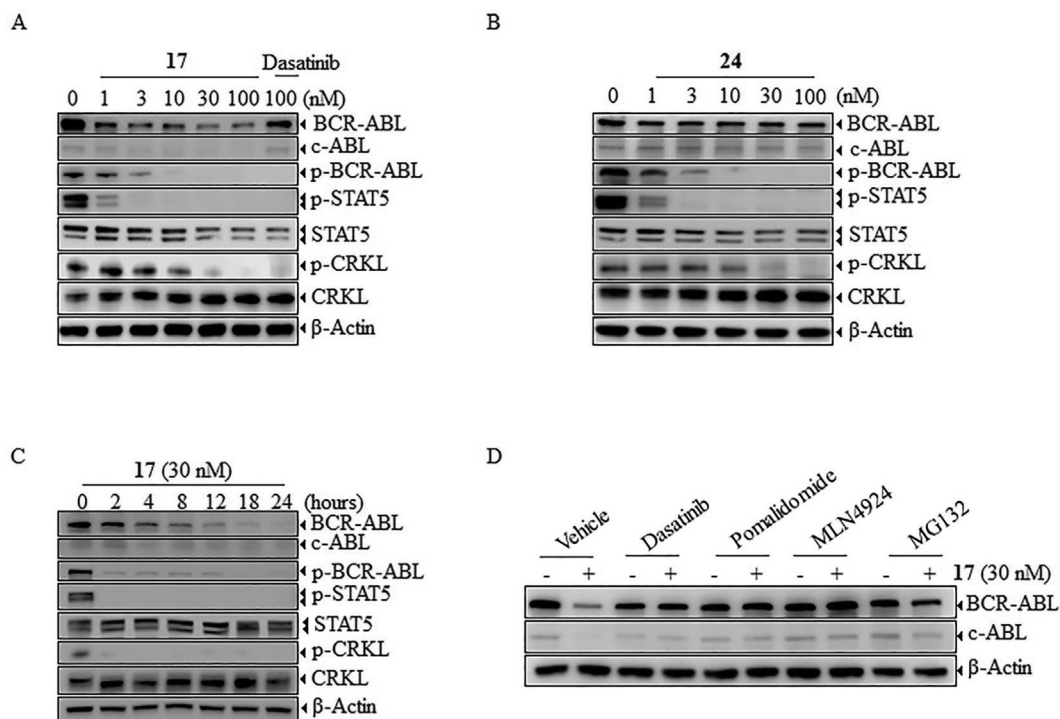


Fig. 4. The BCR-ABL degradation induced by the degrader **17**. (A, B) K562 cells were treated for 16 h with **17** or **24** at different concentrations, and dasatinib was included as control compound. The protein levels were analyzed by western blotting. (C) K562 cells were treated with **17** for time as indicated. The BCR-ABL and c-ABL protein levels were determined by Western blot. (D) K562 cells were pretreated with DMSO, pomalidomide (4  $\mu$ M), dasatinib (100 nM), proteasome inhibitors MG132 (2  $\mu$ M) or NEDD8-activating enzyme (NAE) inhibitor MLN4924 (3  $\mu$ M) for 2 h and then followed by **17** treatment at 30 nM for 8 h.

dasatinib resistance [41–43]. As depicted in Fig. 5, besides of degradation on wide-type BCR-ABL, degrader **17** also induced degradation of BCR-ABL mutations, including G250E, E255V, V299L, F317L, F317V and T315A at low nanomolar concentration. However, the T315I mutant resulting from gatekeeper T315 residue replacement with isoleucine, which sterically blocked the critical direct binding with imatinib and dasatinib examined by the crystal structure study [44], were as expectedly refractory to **17**-induced degradation.

### 2.2.5. Anti-leukemic efficacy of **17** in vivo

Next, we then evaluated the tolerability and anti-CML efficacy of **17** in a murine xenograft model of K562 cells exogenously carrying a luciferase reporter gene (termed K562-Luc) with dasatinib as control compound. After 10 days of treatment, intraperitoneal administration of **17** alleviated tumor progression in a dose-dependent manner as determined by serial volumetric measurement (Fig. 6A). A decrease in tumor burden was observed in degrader **17**-treated mice at 1 mg/kg and the complete tumor regression was induced following injections of **17** at 10 mg/kg, which was maintained even after drug withdrawal. The tumor growth inhibition (TGI) is calculated at day 10 and shows values of

78.9%, 93.8%, and 98.8% for the 1, 3, and 10 mg/kg dosages of degrader **17**, respectively. Of note, **17** at 3 mg/kg by intraperitoneal administration exhibited similar anti-leukemic activity to that of dasatinib at 5 mg/kg by oral administration (TGI: 93.8% versus 95.1%), although the comparison may be not so rational according to the differences of administration methods and physicochemical properties between the two compounds. Notably, the mice were well tolerated even given compound **17** at the dose of 100 mg/kg (data not shown) and the animal weight was preserved during the treatment procedure above (Fig. 6B). The *in vivo* anti-CML efficacy of **17** was further confirmed by bioluminescence imaging after 10 days of treatment (Fig. 6C and D). All the results indicated that **17** exerted potent activity and safety *in vivo*. Moreover, the BCR-ABL protein degradation was also observed following the daily continuous 4 days' treatment, paralleled by suppression of BCR-ABL phosphorylation (Supporting Fig. S4). Taken together, the results clarified that PROTAC **17** induced effective degradation of BCR-ABL protein and substantial anti-leukemic activity *in vivo*.

### 3. Conclusion

PROTACs represent a novel strategy for therapeutic

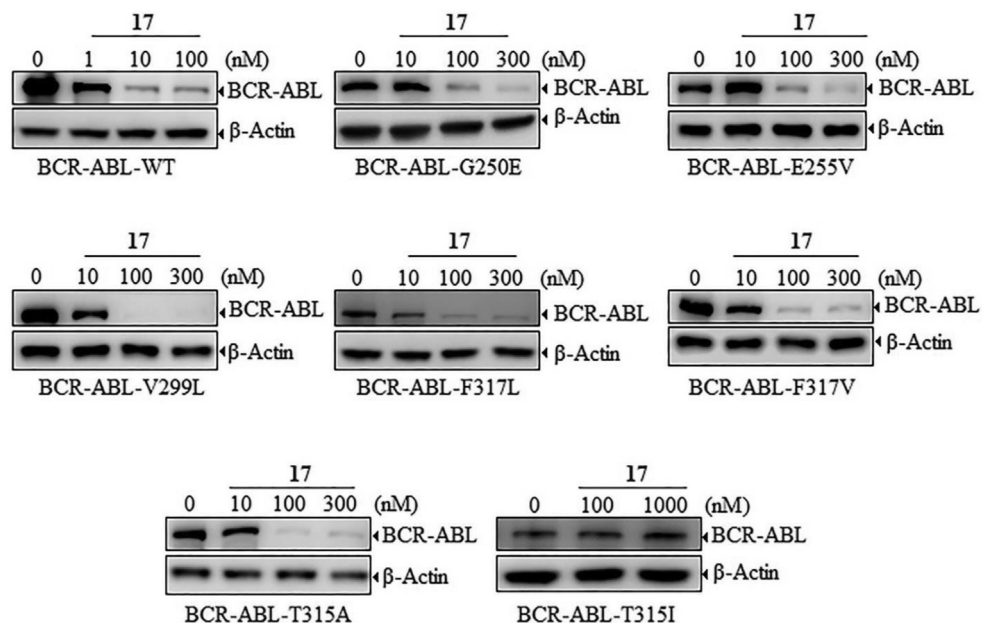


**Fig. 5.** The degradative activity of **17** against BCR-ABL mutations. The western blotting analysis of wide-type and mutant isoforms of BCR-ABL exogenously expressed in 32D cells following treatment of **17** at different concentrations.

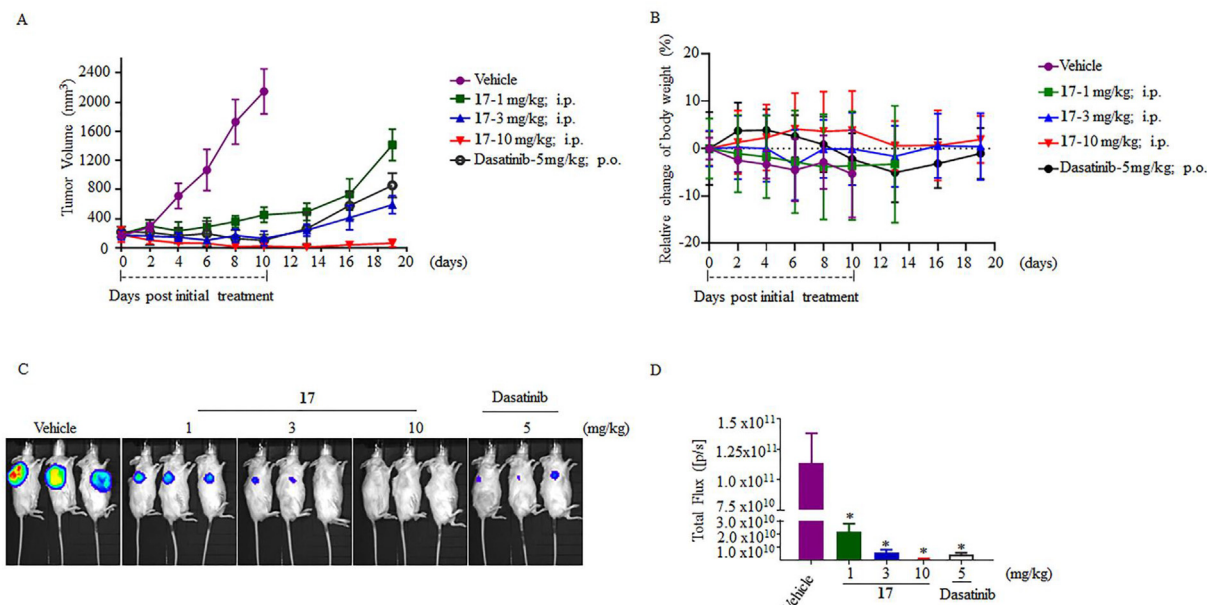


**Fig. 6.** *In vivo* anti-leukemic efficacy of BCR-ABL degrader **17** in the K562-Luc xenograft models. (A) The tumor volume was measured following intraperitoneal administration of **17** (IP) at different dose-schedules. Administration of dasatinib (PO) was served as controls. The dashed-line indicates the treatment period. (B) The body weight alteration was measured following treatment as indicated. (C) Tumor burden was monitored by measuring the luciferase activity through bioluminescence imaging. (D) Quantitative results were analyzed for each group ( $n \geq 6$ ) and expressed as total photon values per second (Total Flux [p/s]). The symbols \* indicate  $P < 0.05$  compared with the vehicle-treated group.

intervention. The lingering problem of BCR-ABL-targeted therapy such as persistent leukemic stem cells retention and resistance-conferring mutations urge the exploration of potential BCR-ABL degraders. In this study, we attempt to design novel BCR-ABL degraders by conjugating BCR-ABL inhibitor dasatinib and CRBN ligands and perform SAR studies to identify the potent and selective PROTACs targeting BCR-ABL. We focused on the extensive optimization of linkers' parameters and our results showed that pomalidomide-based degrader **17** (SIAIS056), exerted the most

potent BCR-ABL-degrading activity *in vitro* and favorable pharmacokinetics *in vivo*. Besides, degrader **17** also degrades several clinically relevant resistance-conferring mutations of BCR-ABL except for T315I. Moreover, degrader **17** induces BCR-ABL degradation and significant tumor regression against K562 xenograft tumors *in vivo*. Our study indicates that **17** as an efficacious BCR-ABL degrader warrants extensive further investigation for the treatment of BCR-ABL<sup>+</sup> leukemia.

## 4. Experimental protocols

### 4.1. Chemistry

All chemicals were obtained from commercial suppliers (Adamas and Alfa), and used without further purification, unless otherwise indicated. Flash chromatography was carried out on silica gel (200–300 mesh). Analytical TLC was performed on Haiyang ready-to-use plates with silica gel 60 (F254). All new compounds were characterized by  $^1\text{H}$  NMR and  $^{13}\text{C}$  NMR, HRMS.  $^1\text{H}$  NMR spectra were recorded on Bruker AVANCE III 500 MHz (operating at 500 MHz for  $^1\text{H}$  NMR), chemical shifts were reported in ppm relative to the residual DMSO- $d_6$  (2.50 ppm  $^1\text{H}$ ), and coupling constants (J) are given in Hz. Multiplicities of signals are described as follows: s = singlet, d = doublet, t = triplet, q = quartet, m = multiple. High Resolution Mass spectra were recorded on AB Triple 4600 spectrometer with acetonitrile and water as solvent. The final compounds were all purified by C18 reverse phase preparative HPLC column with solvent A (0.05% HCl in  $\text{H}_2\text{O}$ ) and solvent B (MeCN) as eluents. The purity of all the final compounds was confirmed to be >95% purity by HPLC (SHIMADZU).

#### 4.1.1. *N*-(2-chloro-6-methylphenyl)-2-((2-methyl-6-(piperazin-1-yl)pyrimidin-4-yl)amino)thiazole-5-carboxamide (**S2**)

In a round-bottom flask, to a stirred solution of compound **S1** (1.0 g, 2.54 mmol) in *n*-butyl alcohol (20 ml) DIPEA (4.9 g, 38 mmol) and piperazine (0.55 g, 6.35 mmol) were added. Then the resulting mixture was stirred for 16 h at 110 °C under the nitrogen atmosphere. Once the starting material disappeared, monitored by LCMS, the mixture was filtered through Celite and washed with MeOH. The collected solid was then added to a round-bottom flask which was equipped with water (10 ml) and MeOH (30 ml). Then the mixture was stirred for another 1 h at 60 °C. The solid was collected by filtration and washed with MeOH to furnish compound **S2** as a white solid (0.9 g, yield 80%).  $^1\text{H}$  NMR (500 MHz, DMSO- $d_6$ )  $\delta$  9.88 (s, 1H), 8.23 (s, 1H), 7.43–7.38 (m, 1H), 7.31–7.24 (m, 2H), 6.04 (s, 1H), 3.45 (d,  $J$  = 4.6 Hz, 4H), 2.79–2.71 (m, 4H), 2.44–2.37 (m, 3H), 2.25 (s, 3H). HRMS (ESI)  $\text{C}_{20}\text{H}_{23}\text{ClN}_7\text{OS}^+$  [M + H] $^+$ , calcd 444.1368; found, 444.1361.

#### 4.1.2. 3-(2-((2-(2,6-dioxopiperidin-3-yl)-1,3-dioxoisindolin-4-yl)amino)ethoxy)propanoic acid (**S5-1**)

2-(2,6-dioxopiperidin-3-yl)-4-fluoroisindoline-1,3-dione (5 mmol, 1equiv), *tert*-butyl 3-(2-aminoethoxy)propanoate (6 mmol, 1.2 equiv) and DIPEA (25 mmol, 5 equiv) were put into the microwave reaction tube (30 ml), then added 8 ml NMP. And the tube was ventilated with argon gas. The reaction mixture was allowed to stir at 110 °C microwave for 2 h. After that, the reaction solution was cooled to room temperature and poured into salt solution. The reaction mixture was further extracted with ethyl acetate (3  $\times$  50 ml). The organic extracts were combined, washed with salt solution (50 ml), dried over  $\text{Na}_2\text{SO}_4$ , filtered, and evaporated under vacuum and was subjected to column purification (PE/EA = 1:1) to furnish the intermediate.

The obtained intermediate was then added to a 50 ml singlet bottle with 88% 20 ml of formic acid and stirred at room temperature for 12 h. The reaction solvent is evaporated and water is added to freeze-dry the final target compound **S5-1**. Yellow solid, 1.0 g, (yield 48%).  $^1\text{H}$  NMR (500 MHz, DMSO- $d_6$ )  $\delta$  12.17 (s, 1H), 11.09 (s, 1H), 7.57 (dd,  $J$  = 8.5, 7.5 Hz, 1H), 7.13 (d,  $J$  = 8.6 Hz, 1H), 7.04 (d,  $J$  = 7.0 Hz, 1H), 6.59 (t,  $J$  = 5.7 Hz, 1H), 5.05 (dd,  $J$  = 12.8, 5.4 Hz, 1H), 3.65 (t,  $J$  = 6.3 Hz, 2H), 3.59 (t,  $J$  = 5.5 Hz, 2H), 3.46 (q,  $J$  = 5.5 Hz, 2H), 2.91–2.83 (m, 1H), 2.61–2.52 (m, 2H), 2.46 (t,  $J$  = 6.3 Hz, 2H), 2.05–2.00 (m, 1H). MS (ESI,  $m/z$ ): 390 [M+H] $^+$ .

#### 4.1.3. *N*-(2-chloro-6-methylphenyl)-2-((6-(4-(3-(2-((2-(2,6-dioxopiperidin-3-yl)-1,3-dioxo isoindolin-4-yl)amino)ethoxy)propanoyl)piperazin-1-yl)-2-methylpyrimidin-4-yl)amino)thiazole-5-carboxamide (**4**)

Compound **S2** (1.2 mmol, 1 equiv) and compound **S5-1** (1.2 mmol) were added into a dry round-bottom flask. Then HOAt (1.8 mmol, 1.5 equiv), EDCI (1.8 mmol, 1.5 equiv), NMM (2.4 mmol, 2 equiv) and DMF (3 ml) were mixed and stirred at 25 °C for 12 h. The reaction was quenched with water (1.0 ml) followed by purification via preparative HPLC (100 g, C18 column) to afford the desired product **4**. Yellow solid, 30.2 mg, (yield 82%).  $^1\text{H}$  NMR (500 MHz,  $\text{CD}_3\text{OD}$ )  $\delta$  8.21 (s, 1H), 7.55–7.47 (m, 1H), 7.37 (dd,  $J$  = 7.5, 1.5 Hz, 1H), 7.30–7.21 (m, 2H), 7.04 (d,  $J$  = 8.5 Hz, 1H), 6.95 (d,  $J$  = 7.1 Hz, 1H), 6.13 (s, 1H), 5.02 (dd,  $J$  = 12.8, 5.4 Hz, 1H), 3.84 (t,  $J$  = 5.8 Hz, 2H), 3.79–3.62 (m, 10H), 3.52–3.45 (m, 2H), 2.87–2.79 (m, 1H), 2.77–2.61 (m, 4H), 2.54 (s, 3H), 2.33 (s, 3H), 2.13–2.05 (m, 1H).  $^{13}\text{C}$  NMR (126 MHz, DMSO- $d_6$ )  $\delta$  172.79, 170.08, 168.97 (d,  $J$  = 4.0 Hz), 167.26, 165.16, 162.53, 162.14, 159.91, 156.93, 146.39, 140.83, 138.83, 136.25, 133.52, 132.44, 132.08, 129.04, 128.19, 127.02, 125.78, 117.42, 110.68, 109.23, 82.75, 68.70, 66.70, 48.57, 44.30, 43.52, 43.17, 41.69, 40.50, 32.82, 30.98, 25.53, 22.16, 18.31. MS (ESI,  $m/z$ ): 815 [M+H] $^+$ .

#### 4.1.4. 3-(2-((2-(2-(2,6-dioxopiperidin-3-yl)-1,3-dioxoisindolin-4-yl)amino)ethoxy)ethoxy)propanoic acid (**S5-2**)

The synthesis of intermediate **S5-2** was similar to **S5-1**. Yellow solid, 0.95 g, (yield 51%).  $^1\text{H}$  NMR (500 MHz, DMSO- $d_6$ )  $\delta$  11.09 (s, 1H), 7.58 (dd,  $J$  = 8.0, 7.5 Hz, 1H), 7.14 (d,  $J$  = 8.6 Hz, 1H), 7.04 (d,  $J$  = 7.0 Hz, 1H), 6.60 (t,  $J$  = 5.7 Hz, 1H), 5.05 (dd,  $J$  = 12.8, 5.4 Hz, 1H), 3.62–3.58 (m, 4H), 3.56–3.54 (m, 2H), 3.52–3.49 (m, 2H), 3.46 (dd,  $J$  = 11.1, 5.5 Hz, 2H), 2.92–2.84 (m, 1H), 2.66–2.51 (m, 2H), 2.42 (t,  $J$  = 6.4 Hz, 2H), 2.06–1.98 (m, 1H). MS (ESI,  $m/z$ ): 434 [M+H] $^+$ .

#### 4.1.5. *N*-(2-chloro-6-methylphenyl)-2-((6-(4-(3-(2-((2-(2,6-dioxopiperidin-3-yl)-1,3-dioxo isoindolin-4-yl)amino)ethoxy)ethoxy)propanoyl)piperazin-1-yl)-2-methylpyrimidin-4-yl)amino)thiazole-5-carboxamide (**5**)

The derivative **5** was obtained from the condensation of **S5-2** and **S2** according the similar process of **4**. Yellow solid, 13.7 mg, (yield 35%).  $^1\text{H}$  NMR (500 MHz,  $\text{CD}_3\text{OD}$ )  $\delta$  8.18 (s, 1H), 7.49–7.43 (m, 1H), 7.38–7.34 (m, 1H), 7.29–7.21 (m, 2H), 6.97 (d,  $J$  = 8.6 Hz, 1H), 6.92 (d,  $J$  = 7.1 Hz, 1H), 6.09 (s, 1H), 5.05 (dd,  $J$  = 12.7, 5.5 Hz, 1H), 3.79 (t,  $J$  = 5.8 Hz, 4H), 3.70 (dd,  $J$  = 11.6, 6.3 Hz, 6H), 3.64 (t,  $J$  = 3.8 Hz, 6H), 3.42 (t,  $J$  = 5.2 Hz, 2H), 2.89–2.79 (m, 1H), 2.78–2.65 (m, 4H), 2.50 (s, 3H), 2.33 (s, 3H), 2.15–2.09 (m, 1H).  $^{13}\text{C}$  NMR (126 MHz, DMSO- $d_6$ )  $\delta$  172.81, 170.10, 169.13, 168.96, 167.28, 165.07, 162.52, 162.03, 159.89, 156.90, 146.39, 140.81, 138.83, 136.21, 133.50, 132.44, 132.08, 129.05, 128.20, 127.03, 125.76, 117.43, 110.67, 109.25, 82.79, 69.74, 68.88, 66.86, 48.57, 44.31, 43.58, 43.25, 41.71, 40.47, 32.88, 30.99, 25.46, 22.15, 18.31. MS (ESI,  $m/z$ ): 859 [M+H] $^+$ .

#### 4.1.6. 3-(2-((2-((2-(2,6-dioxopiperidin-3-yl)-1,3-dioxoisindolin-4-yl)amino)ethoxy)ethoxy)ethoxy)propanoic acid (**S5-3**)

The synthesis of intermediate **S5-3** was similar to **S5-1**. Yellow solid, 0.95 g, (yield 61%).  $^1\text{H}$  NMR (500 MHz, DMSO- $d_6$ )  $\delta$  11.09 (s, 1H), 7.58 (dd,  $J$  = 8.0, 7.0 Hz, 1H), 7.15 (d,  $J$  = 8.6 Hz, 1H), 7.04 (d,  $J$  = 7.0 Hz, 1H), 6.61 (t,  $J$  = 5.8 Hz, 1H), 5.05 (dd,  $J$  = 12.8, 5.4 Hz, 1H), 3.63–3.48 (m, 14H), 2.92–2.83 (m, 1H), 2.64–2.52 (m, 2H), 2.18 (t,  $J$  = 8.1 Hz, 2H), 2.07–1.99 (m, 1H). MS (ESI,  $m/z$ ): 478 [M+H] $^+$ .

#### 4.1.7. *N*-(2-chloro-6-methylphenyl)-2-((6-(4-(3-(2-((2-(2,6-dioxopiperidin-3-yl)-1,3-dioxo isoindolin-4-yl)amino)ethoxy)ethoxy)ethoxy)propanoyl)piperazin-1-yl)-2-methylpyrimidin-4-yl)amino)thiazole-5-carboxamide (**6**)

The derivative **6** was obtained from the condensation of **S5-3** and **S2** according the similar process of **4**. Yellow solid, 15.7 mg,

(yield 38%).  $^1\text{H}$  NMR (500 MHz,  $\text{CD}_3\text{OD}$ )  $\delta$  8.17 (s, 1H), 7.54–7.46 (m, 1H), 7.37 (d,  $J = 6.0$  Hz, 1H), 7.29–7.22 (m, 2H), 6.99 (dd,  $J = 14.0$ , 7.8 Hz, 2H), 6.17 (s, 1H), 5.05 (dd,  $J = 12.8$ , 5.5 Hz, 1H), 3.84–3.72 (m, 10H), 3.68 (t,  $J = 5.2$  Hz, 2H), 3.65–3.62 (m, 6H), 3.61–3.59 (m, 2H), 3.43 (t,  $J = 5.2$  Hz, 2H), 2.92–2.81 (m, 1H), 2.77–2.66 (m, 4H), 2.54 (s, 3H), 2.33 (s, 3H), 2.15–2.09 (m, 1H). MS (ESI,  $m/z$ ): 903  $[\text{M}+\text{H}]^+$ .

#### 4.1.8. 1-((2-(2,6-dioxopiperidin-3-yl)-1,3-dioxoisindolin-4-yl)amino)-3,6,9,12-tetraoxapentadecan-15-oic acid (**S5-4**)

The synthesis of intermediate **S5-4** was similar to **S5-1**. Yellow solid, 0.87 g, (yield 53%).  $^1\text{H}$  NMR (500 MHz,  $\text{DMSO}-d_6$ )  $\delta$  11.09 (s, 1H), 7.58 (dd,  $J = 8.5$ , 7.5 Hz, 1H), 7.15 (d,  $J = 8.6$  Hz, 1H), 7.04 (d,  $J = 7.0$  Hz, 1H), 6.60 (t,  $J = 5.7$  Hz, 1H), 5.05 (dd,  $J = 12.8$ , 5.4 Hz, 1H), 3.63–3.48 (m, 18H), 2.92–2.84 (m, 1H), 2.63–2.52 (m, 2H), 2.41 (t,  $J = 6.4$  Hz, 2H), 2.07–1.98 (m, 1H). MS (ESI,  $m/z$ ): 522  $[\text{M}+\text{H}]^+$ .

#### 4.1.9. N-(2-chloro-6-methylphenyl)-2-((6-(4-(1-((2-(2,6-dioxopiperidin-3-yl)-1,3-dioxoisindolin-4-yl)amino)-3,6,9,12-tetraoxapentadecan-15-oyl)piperazin-1-yl)-2-methylpyrimidin-4-yl)amino)thiazole-5-carboxamide (**7**)

The derivative **7** was obtained from the condensation of **S5-4** and **S2** according the similar process of **4**. Yellow solid, 18.6 mg, (yield 43%).  $^1\text{H}$  NMR (500 MHz,  $\text{CD}_3\text{OD}$ )  $\delta$  8.17 (s, 1H), 7.50 (t,  $J = 7.8$  Hz, 1H), 7.36 (d,  $J = 7.2$  Hz, 1H), 7.31–7.21 (m, 2H), 7.06–6.95 (m, 2H), 6.19 (s, 1H), 5.05 (dd,  $J = 12.8$ , 5.5 Hz, 1H), 3.85–3.71 (m, 10H), 3.70 (t,  $J = 5.2$  Hz, 2H), 3.66–3.57 (m, 12H), 3.44 (t,  $J = 5.0$  Hz, 2H), 2.90–2.82 (m, 1H), 2.76–2.65 (m, 4H), 2.55 (s, 3H), 2.33 (s, 3H), 2.16–2.07 (m, 1H).  $^{13}\text{C}$  NMR (126 MHz,  $\text{DMSO}-d_6$ )  $\delta$  172.82, 170.09, 169.13, 168.95, 167.30, 165.08, 162.54, 162.04, 159.89, 156.92, 146.41, 140.77, 138.83, 136.22, 133.51, 132.44, 132.09, 129.05, 128.21, 127.03, 125.80, 117.44, 110.68, 109.25, 82.82, 69.89–69.67 (m), 68.89, 66.78, 48.57, 44.32, 43.61, 43.28, 41.70, 40.47, 32.87, 30.99, 25.45, 22.16, 18.31. MS (ESI,  $m/z$ ): 947  $[\text{M}+\text{H}]^+$ .

#### 4.1.10. 1-((2-(2,6-dioxopiperidin-3-yl)-1,3-dioxoisindolin-4-yl)amino)-3,6,9,12,15-pentaoxa octadecan-18-oic acid (**S5-5**)

The synthesis of intermediate **S5-5** was similar to **S5-1**. Yellow solid, 0.8 g, (yield 51%).  $^1\text{H}$  NMR (500 MHz,  $\text{DMSO}-d_6$ )  $\delta$  11.09 (s, 1H), 7.58 (t,  $J = 8.0$  Hz, 1H), 7.14 (d,  $J = 8.6$  Hz, 1H), 7.04 (d,  $J = 7.0$  Hz, 1H), 6.60 (t,  $J = 5.7$  Hz, 1H), 5.05 (dd,  $J = 12.8$ , 5.4 Hz, 1H), 3.63–3.54 (m, 8H), 3.54–3.48 (m, 12H), 3.30 (dd,  $J = 7.0$  Hz, 4H), 2.92–2.84 (m, 1H), 2.63–2.52 (m, 2H), 2.06–1.99 (m, 1H). MS (ESI,  $m/z$ ): 947  $[\text{M}+\text{H}]^+$ .

#### 4.1.11. N-(2-chloro-6-methylphenyl)-2-((6-(4-(1-((2-(2,6-dioxopiperidin-3-yl)-1,3-dioxoisindolin-4-yl)amino)-3,6,9,12,15-pentaoxa octadecan-18-oyl)piperazin-1-yl)-2-methylpyrimidin-4-yl)amino)thiazole-5-carboxamide (**8**)

The derivative **8** was obtained from the condensation of **S5-5** and **S2** according the similar process of **4**. Yellow solid, 35 mg, (yield 78%).  $^1\text{H}$  NMR (500 MHz,  $\text{CD}_3\text{OD}$ )  $\delta$  8.18 (s, 1H), 7.54–7.48 (m, 1H), 7.36 (d,  $J = 7.4$  Hz, 1H), 7.28–7.22 (m, 2H), 7.03 (dd,  $J = 16.0$ , 7.8 Hz, 2H), 6.23 (s, 1H), 5.04 (dd,  $J = 12.8$ , 5.4 Hz, 1H), 3.86–3.73 (m, 10H), 3.71 (t,  $J = 5.1$  Hz, 2H), 3.78–3.68 (m, 10H), 3.65–3.60 (m, 7H), 3.59–3.57 (m, 9H), 3.46 (t,  $J = 5.1$  Hz, 2H), 2.89–2.81 (m, 1H), 2.76–2.65 (m, 4H), 2.57 (s, 3H), 2.32 (s, 3H), 2.15–2.08 (m, 1H).  $^{13}\text{C}$  NMR (126 MHz,  $\text{DMSO}-d_6$ )  $\delta$  173.27, 170.54, 169.58, 169.40, 167.76, 165.58, 162.98, 162.54, 160.35, 157.39, 146.88, 141.25, 139.29, 136.69, 133.96, 132.90, 132.55, 129.51, 128.67, 127.49, 126.26, 117.91, 111.14, 109.70, 83.27, 70.48–69.97 (m), 69.35, 67.25, 49.03, 44.77, 44.05, 43.73, 42.16, 40.93, 33.33, 31.45, 25.94, 22.61, 18.76. MS (ESI,  $m/z$ ): 947  $[\text{M}+\text{H}]^+$ .

#### 4.1.12. 4-((2-(2,6-dioxopiperidin-3-yl)-1,3-dioxoisindolin-4-yl)amino)butanoic acid (**S7-1**)

The synthesis of intermediate **S7-1** was similar to **S5-1**. Yellow solid, 0.8 g, (yield 61%).  $^1\text{H}$  NMR (500 MHz,  $\text{DMSO}-d_6$ )  $\delta$  12.14 (s, 1H), 11.09 (s, 1H), 7.58 (dd,  $J = 8.4$ , 7.3 Hz, 1H), 7.13 (d,  $J = 8.6$  Hz, 1H), 7.02 (d,  $J = 7.0$  Hz, 1H), 6.65 (t,  $J = 6.0$  Hz, 1H), 5.05 (dd,  $J = 12.8$ , 5.4 Hz, 1H), 3.32 (dd,  $J = 13.7$ , 6.7 Hz, 2H), 2.94–2.82 (m, 1H), 2.66–2.51 (m, 2H), 2.30 (t,  $J = 7.2$  Hz, 2H), 2.05–2.00 (m, 1H), 1.82–1.75 (m, 2H). MS (ESI,  $m/z$ ): 360  $[\text{M}+\text{H}]^+$ .

#### 4.1.13. N-(2-chloro-6-methylphenyl)-2-((6-(4-(4-((2-(2,6-dioxopiperidin-3-yl)-1,3-dioxoisindolin-4-yl)amino)butanoyl)piperazin-1-yl)-2-methylpyrimidin-4-yl)amino)thiazole-5-carboxamide (**9**)

The derivative **9** was obtained from the condensation of **S7-1** and **S2** according the similar process of **4**. Yellow solid, 31.2 mg, (yield 88%).  $^1\text{H}$  NMR (500 MHz,  $\text{DMSO}-d_6$ )  $\delta$  11.53 (s, 1H), 11.09 (s, 1H), 9.89 (s, 1H), 8.22 (s, 1H), 7.59 (dd,  $J = 8.5$ , 7.1 Hz, 1H), 7.40 (d,  $J = 7.7$  Hz, 1H), 7.31–7.23 (m, 2H), 7.19 (d,  $J = 8.7$  Hz, 1H), 7.02 (d,  $J = 7.0$  Hz, 1H), 6.68 (s, 1H), 6.07 (s, 1H), 5.05 (dd,  $J = 12.7$ , 5.4 Hz, 1H), 3.51–3.48 (m, 8H), 3.34 (t,  $J = 7.1$  Hz, 2H), 2.92–2.84 (m, 1H), 2.64–2.52 (m, 2H), 2.45 (t,  $J = 7.1$  Hz, 2H), 2.43 (s, 3H), 2.24 (s, 3H), 2.04–2.00 (m, 1H), 1.86–1.79 (m, 2H).  $^{13}\text{C}$  NMR (126 MHz,  $\text{DMSO}-d_6$ )  $\delta$  172.83, 170.50, 170.12, 168.84, 167.33, 165.08, 162.51, 162.03, 159.88, 156.92, 146.41, 140.79, 138.82, 136.25, 133.49, 132.43, 132.25, 129.05, 128.21, 127.02, 125.83, 117.30, 110.41, 109.11, 82.83, 48.54, 44.08, 43.53, 43.28, 41.60, 40.55, 30.99, 29.45, 25.45, 24.16, 22.17, 18.30. MS (ESI,  $m/z$ ): 785  $[\text{M}+\text{H}]^+$ .

#### 4.1.14. 5-((2-(2,6-dioxopiperidin-3-yl)-1,3-dioxoisindolin-4-yl)amino)pentanoic acid (**S7-2**)

The synthesis of intermediate **S7-2** was similar to **S5-1**. Yellow solid, 0.9 g, (yield 50%).  $^1\text{H}$  NMR (500 MHz,  $\text{DMSO}-d_6$ )  $\delta$  12.05 (s, 1H), 11.11 (s, 1H), 7.57 (dd,  $J = 8.3$ , 7.4 Hz, 1H), 7.09 (d,  $J = 8.6$  Hz, 1H), 7.02 (d,  $J = 7.0$  Hz, 1H), 6.56 (t,  $J = 5.9$  Hz, 1H), 5.05 (dd,  $J = 12.7$ , 5.4 Hz, 1H), 3.32–3.28 (m, 2H), 2.94–2.82 (m, 1H), 2.62–2.51 (m, 2H), 2.27–2.25 (m, 2H), 2.06–1.99 (m, 1H), 1.62–1.53 (m, 4H). MS (ESI,  $m/z$ ): 374  $[\text{M}+\text{H}]^+$ .

#### 4.1.15. N-(2-chloro-6-methylphenyl)-2-((6-(4-(5-((2-(2,6-dioxopiperidin-3-yl)-1,3-dioxoisindolin-4-yl)amino)pentanoyl)piperazin-1-yl)-2-methylpyrimidin-4-yl)amino)thiazole-5-carboxamide (**10**)

The derivative **10** was obtained from the condensation of **S7-2** and **S2** according the similar process of **4**. Yellow solid, 10 mg, (yield 28%).  $^1\text{H}$  NMR (500 MHz,  $\text{CD}_3\text{OD}$ )  $\delta$  8.21 (s, 1H), 7.56 (dd,  $J = 8.5$ , 7.2 Hz, 1H), 7.37 (d,  $J = 7.1$  Hz, 1H), 7.26 (t,  $J = 7.7$  Hz, 2H), 7.08 (d,  $J = 8.6$  Hz, 1H), 7.04 (d,  $J = 7.1$  Hz, 1H), 6.30 (s, 1H), 5.04 (dd,  $J = 12.6$ , 5.5 Hz, 1H), 3.83–3.69 (m, 8H), 3.40 (t,  $J = 6.1$  Hz, 2H), 2.89–2.80 (m, 1H), 2.76–2.67 (m, 2H), 2.61 (s, 3H), 2.53 (d,  $J = 6.4$  Hz, 2H), 2.32 (s, 3H), 2.13–2.07 (m, 1H), 1.80–1.72 (m, 4H).  $^{13}\text{C}$  NMR (126 MHz,  $\text{DMSO}-d_6$ )  $\delta$  172.81, 170.76, 170.11, 168.94, 167.30, 163.92, 162.48, 159.73, 158.81, 156.80, 146.41, 139.80 (d,  $J = 250.7$  Hz), 136.27, 133.46, 132.32 (d,  $J = 26.9$  Hz), 129.04, 128.22, 127.03, 117.27, 110.39, 109.04, 83.04, 53.37, 48.54, 43.82 (d,  $J = 63.3$  Hz), 41.60, 31.89, 30.98, 28.30, 22.16, 21.96, 18.31, 18.00, 16.71. MS (ESI,  $m/z$ ): 799  $[\text{M}+\text{H}]^+$ .

#### 4.1.16. 7-((2-(2,6-dioxopiperidin-3-yl)-1,3-dioxoisindolin-4-yl)amino)heptanoic acid (**S7-3**)

The synthesis of intermediate **S7-3** was similar to **S5-1**. Yellow solid, 1.3 g, (yield 64%).  $^1\text{H}$  NMR (500 MHz,  $\text{DMSO}-d_6$ )  $\delta$  12.04 (s, 1H), 11.09 (s, 1H), 7.58 (dd,  $J = 8.3$ , 7.3 Hz, 1H), 7.09 (d,  $J = 8.6$  Hz, 1H), 7.02 (d,  $J = 7.0$  Hz, 1H), 6.53 (t,  $J = 5.9$  Hz, 1H), 5.05 (dd,  $J = 12.7$ , 5.4 Hz, 1H), 3.28 (dd,  $J = 13.4$ , 6.7 Hz, 2H), 2.94–2.82 (m, 1H),

2.65–2.51 (m, 2H), 2.19 (t,  $J = 7.3$  Hz, 2H), 2.05–2.00 (m, 1H), 1.60–1.53 (m, 2H), 1.53–1.46 (m, 2H), 1.37–1.28 (m, 4H). MS (ESI,  $m/z$ ): 799  $[M+H]^+$ .

4.1.17. *N*-(2-chloro-6-methylphenyl)-2-((6-(4-(7-((2-(2,6-dioxopiperidin-3-yl)-1,3-dioxoisindolin-4-yl)amino)heptanoyl)piperazin-1-yl)-2-methylpyrimidin-4-yl)amino)thiazole-5-carboxamide (**11**)

The derivative **11** was obtained from the condensation of **S7-3** and **S2** according the similar process of **4**. Yellow solid, 10 mg, (yield 28%).  $^1\text{H}$  NMR (500 MHz,  $\text{CD}_3\text{OD}$ )  $\delta$  7.54 (dd,  $J = 8.5, 7.1$  Hz, 1H), 7.36 (d,  $J = 6.1$  Hz, 1H), 7.28–7.22 (m, 3H), 7.03 (dd,  $J = 10.7, 7.8$  Hz, 2H), 6.15 (s, 1H), 5.04 (dd,  $J = 12.6, 5.5$  Hz, 1H), 3.89–3.62 (m, 8H), 3.34 (t,  $J = 7.5$  Hz, 2H), 2.87–2.80 (m, 1H), 2.77–2.68 (m, 2H), 2.56 (s, 3H), 2.45 (t,  $J = 7.5$  Hz, 2H), 2.32 (s, 3H), 2.13–2.08 (m, 1H), 1.72–1.64 (m, 4H), 1.53–1.39 (m, 4H).  $^{13}\text{C}$  NMR (126 MHz,  $\text{DMSO}-d_6$ )  $\delta$  172.80, 170.87, 170.09, 168.94, 167.43, 167.29, 161.24, 159.55, 158.50, 156.90, 146.42, 140.81, 138.77, 136.28, 133.30, 132.38, 132.19, 129.06, 128.29, 127.03, 117.18, 110.37, 109.00, 103.44, 83.00, 48.52, 44.35, 43.64, 43.11, 41.79, 40.42, 32.20, 30.96, 28.53 (d,  $J = 11.3$  Hz), 26.16, 25.16, 24.64, 22.14, 18.28 (d,  $J = 2.4$  Hz). MS (ESI,  $m/z$ ): 827  $[M+H]^+$ .

4.1.18. 2-(2,6-dioxopiperidin-3-yl)-4-mercaptoisindoline-1,3-dione (**S8**)

Compound **S3** (20 g, 72.4 mmol) was dissolved in DMF (150 ml) at room temperature, then  $\text{Na}_2\text{S} \cdot 9\text{H}_2\text{O}$  (28 g, 108.6 mmol) was added and the mixture were stirred for 3 h. After that the reaction solution were poured into ice water (400 ml), and adjust the pH to 2–3 at 6 N HCl solution. The white solid was precipitated. Filter cake was washed with water for 3 times, then beaten with 100 mL anhydrous acetone, and filtered. The filter cake was washed with acetone for 3 times to afford hoary solid **S8**, 14 g, 67%.  $^1\text{H}$  NMR (500 MHz,  $\text{DMSO}-d_6$ )  $\delta$  11.16 (s, 1H), 7.79 (d,  $J = 7.8$  Hz, 1H), 7.69 (t,  $J = 7.6$  Hz, 1H), 7.64 (d,  $J = 7.1$  Hz, 1H), 6.30 (s, 1H), 5.14 (dd,  $J = 12.9, 5.4$  Hz, 1H), 2.93–2.84 (m, 1H), 2.62–2.52 (m, 2H), 2.09–2.02 (m, 1H). MS (ESI,  $m/z$ ): 291  $[M+H]^+$ .

4.1.19. *tert*-butyl 2-((2-(2,6-dioxopiperidin-3-yl)-1,3-dioxoisindolin-4-yl)thio)acetate (**S9**)

The compound **S8** (1.0 g, 3.5 mmol) was added to a 100 ml bottle, followed by anhydrous DMF (10 ml) and anhydrous  $\text{K}_2\text{CO}_3$  (0.97 g, 7.0 mmol). Then *tert*-butyl bromoacetate (0.82 g, 4.2 mmol) was added slowly and stirred at room temperature for 0.5 h. Water (50 ml) was poured into the reaction mixture which was extracted with EA ( $2 \times 50$  ml), and washed with water ( $3 \times 20$  ml), saturated salt solution (50 ml), then dried over  $\text{Na}_2\text{SO}_4$ , filtered, and evaporated under vacuum and was subjected to column purification (DCM/EA = 20:1) to furnish the intermediate **S9**. Light yellow, 1.1 g, (yield 79%).  $^1\text{H}$  NMR (500 MHz,  $\text{DMSO}-d_6$ )  $\delta$  11.13 (s, 1H), 7.80 (dd,  $J = 8.1, 7.3$  Hz, 1H), 7.67 (dd,  $J = 7.6, 4.8$  Hz, 2H), 5.13 (dd,  $J = 12.9, 5.4$  Hz, 1H), 4.07 (s, 2H), 2.94–2.83 (m, 1H), 2.65–2.51 (m, 2H), 2.09–2.04 (m, 1H), 1.39 (s, 9H). MS (ESI,  $m/z$ ): 349  $[M+H]^+$ .

4.1.20. 2-((2-(2,6-dioxopiperidin-3-yl)-1,3-dioxoisindolin-4-yl)thio)acetic acid (**S10**)

The compound **S9** (1.0 g, 2.5 mmol) was added to a 25 ml bottle, followed by 88% formic acid (10 ml) and stirred at room temperature for 12 h. After evaporated the solvent, water was added and the residue was freeze-drying to afford the crude product (**S10**), pale yellow solid, 0.69 g, (yield 80%).  $^1\text{H}$  NMR (500 MHz,  $\text{DMSO}-d_6$ )  $\delta$  13.06 (s, 1H), 11.15 (s, 1H), 7.80 (dd,  $J = 8.1, 7.3$  Hz, 1H), 7.66 (t,  $J = 7.9$  Hz, 2H), 5.13 (dd,  $J = 12.9, 5.4$  Hz, 1H), 4.09 (s, 2H), 2.92–2.85 (m, 1H), 2.66–2.51 (m, 2H), 2.08–2.03 (m, 1H). MS (ESI,  $m/z$ ): 349  $[M+H]^+$ .

4.1.21. *N*-(2-chloro-6-methylphenyl)-2-((6-(4-(2-((2-(2,6-dioxopiperidin-3-yl)-1,3-dioxoisindolin-4-yl)thio)acetyl)piperazin-1-yl)-2-methylpyrimidin-4-yl)amino)thiazole-5-carboxamide (**12**)

Compounds **S2** (27.2 mg, 0.06 mmol), **S10** (20 mg, 0.06 mmol), HOAt (16.3 mg, 0.12 mmol), EDCI (23 mg, 0.12 mmol), anhydrous DMF (2 mL), and NMM (30 mg, 0.30 mmol) were added to the reaction bottle and stirred overnight at room temperature. The reaction was quenched with water (1.0 ml) followed by purification via preparative HPLC (100 g, C18 column) to afford the desired product **12**. Yellow solid, 26.6 mg, (yield 56%).  $^1\text{H}$  NMR (500 MHz,  $\text{DMSO}-d_6$ )  $\delta$  11.56 (s, 1H), 11.15 (s, 1H), 9.91 (s, 1H), 8.23 (s, 1H), 7.85–7.75 (m, 2H), 7.64 (d,  $J = 6.4$  Hz, 1H), 7.40 (d,  $J = 7.2$  Hz, 1H), 7.34–7.21 (m, 2H), 6.09 (s, 1H), 5.13 (dd,  $J = 12.9, 5.4$  Hz, 1H), 4.34 (s, 2H), 3.75–3.59 (m, 8H), 2.94–2.84 (m, 1H), 2.64–2.53 (m, 2H), 2.44 (s, 3H), 2.24 (s, 3H), 2.10–2.02 (m, 1H).  $^{13}\text{C}$  NMR (126 MHz,  $\text{DMSO}-d_6$ )  $\delta$  172.79, 169.89, 166.69 (d,  $J = 6.8$  Hz), 165.77, 165.24, 162.51, 162.24, 159.91, 156.99, 140.86, 138.82, 138.34, 134.81, 133.51, 132.36 (d,  $J = 20.2$  Hz), 131.29, 129.04, 128.19, 127.02, 125.79, 125.34, 119.07, 82.86, 48.92, 44.68, 43.28 (d,  $J = 49.7$  Hz), 41.17, 33.39, 30.95, 25.59, 21.96, 18.31. HRMS (ESI)  $m/z$ : calcd  $\text{C}_{35}\text{H}_{33}\text{ClN}_9\text{O}_6\text{S}_2^+$   $[M+H]^+$ , 774.1678; found, 774.1688.

4.1.22. 2-(2,6-dioxopiperidin-3-yl)-1,3-dioxoisindolin-4-yl glycine (**S7-4**)

The synthesis of intermediate **S7-4** was similar to **S5-1**. Yellow solid, 1.2 g, (yield 48%).  $^1\text{H}$  NMR (500 MHz,  $\text{DMSO}-d_6$ )  $\delta$  11.10 (s, 1H), 7.59 (dd,  $J = 15.9, 8.5$  Hz, 1H), 7.07 (d,  $J = 7.0$  Hz, 1H), 6.99 (d,  $J = 8.6$  Hz, 1H), 6.86 (t,  $J = 5.7$  Hz, 1H), 5.06 (dt,  $J = 15.1, 7.6$  Hz, 1H), 4.08 (d,  $J = 5.7$  Hz, 2H), 2.92–2.84 (m, 1H), 2.63–2.52 (m, 2H), 2.07–2.02 (m, 1H). MS (ESI,  $m/z$ ): 322  $[M+H]^+$ .

4.1.23. *N*-(2-chloro-6-methylphenyl)-2-((6-(4-((2-(2,6-dioxopiperidin-3-yl)-1,3-dioxoisindolin-4-yl)glycyl)piperazin-1-yl)-2-methylpyrimidin-4-yl)amino)thiazole-5-carboxamide (**13**)

The derivative **13** was obtained from the condensation of **S7-4** and **S2** according the similar process of **4**. Yellow solid, 19.1 mg, (yield 56%).  $^1\text{H}$  NMR (500 MHz,  $\text{CD}_3\text{OD}$ )  $\delta$  8.11 (s, 1H), 7.51–7.46 (m, 1H), 7.27 (d,  $J = 7.9$  Hz, 1H), 7.19–7.12 (m, 2H), 7.01 (d,  $J = 7.0$  Hz, 1H), 6.94 (d,  $J = 8.5$  Hz, 1H), 6.19 (s, 1H), 4.98 (dd,  $J = 12.6, 5.3$  Hz, 1H), 4.19 (s, 2H), 3.83–3.63 (m, 8H), 2.82–2.73 (m, 1H), 2.69–2.61 (m, 2H), 2.50 (s, 3H), 2.22 (s, 3H), 2.06–1.99 (m, 1H).  $^{13}\text{C}$  NMR (126 MHz,  $\text{DMSO}-d_6$ )  $\delta$  172.83, 170.09, 168.83, 167.36, 166.73, 165.18, 162.52, 162.14, 159.90, 156.99, 145.48, 138.83, 136.21, 133.50, 132.44, 132.04, 129.05, 128.20, 127.03, 125.82, 118.21, 110.88, 109.60, 82.91, 48.60, 43.73, 43.19 (d,  $J = 28.1$  Hz), 41.06, 31.00, 25.53, 22.16, 18.30. MS (ESI,  $m/z$ ): 757  $[M+H]^+$ .

4.1.24. 2-(2,6-dioxopiperidin-3-yl)-4-hydroxyisindoline-1,3-dione (**S14**)

4-hydroxyisobenzofuran-1,3-dione **S13** (500 mg, 3.05 mmol), 3-aminopiperidine-2, 6-dione (502 mg, 3.05 mmol) and triethylamine (340 mg, 3.36 mmol) were added to a 100 ml egg-shaped bottle, followed by anhydrous toluene (20 mL). The reaction solution was then slowly raised to 110 °C and stirred for 12 h. After that, the reaction solution was reduced to room temperature, and a large number of white and brown solids were precipitated. Filtrated, the filter cake was added to the egg-shaped bottle containing 30% water (10 mL) and methanol (2 mL), and washed with ethyl acetate/petroleum ether for stirring 0.25 h. After filtrated, the filter cake was washed with petroleum ether to drying compound **S14**, white solid, 770 mg, (yield 92%).  $^1\text{H}$  NMR (500 MHz,  $\text{DMSO}-d_6$ )  $\delta$  11.17 (s, 1H), 11.08 (s, 1H), 7.65 (dd,  $J = 8.3, 7.3$  Hz, 1H), 7.32 (d,  $J = 7.1$  Hz, 1H), 7.25 (d,  $J = 8.3$  Hz, 1H), 5.07 (dd,  $J = 12.8, 5.4$  Hz, 1H), 2.92–2.85 (m, 1H), 2.62–2.51 (m, 2H), 2.07–1.96 (m,

1H). MS (ESI,  $m/z$ ): 275  $[M+H]^+$ .

4.1.25. 2-((2-(2,6-dioxopiperidin-3-yl)-1,3-dioxoisindolin-4-yl)oxy)acetic acid (**S16**)

The compound **S14** (412 mg, 1.50 mmol), *tert*-butyl bromide (350 mg, 1.80 mmol), anhydrous sodium bicarbonate (190 mg, 2.25 mmol), potassium iodide (25 mg, 0.15 mmol) and anhydrous DMF (10 mL) were added to a 50 ml egg-shaped bottle and slowly raised to 60 °C and stirred for 12 h. After that, water was added to the reaction bottle. The reaction mixture was extracted with ethyl acetate, and washed with saturated salt solution, dried with anhydrous sodium sulfate. After evaporated the solvent, the compound was purified by column chromatography (eluent: 40% EA/PE) to get **S15** with a pale yellow solid, 520 mg, (yield 89%).

The obtained intermediate **S15** (500 mg, 1.29 mmol), TFA (2 mL) and anhydrous dichloromethane (10 mL) were added to a 50 mL egg-shaped bottle and stirred for 2 h at room temperature. After that, the reaction solvent was removed by decompression, and the crude product was prepared by C18 reversed phase column to afford compound (**S16**) with a white solid, 400 mg, (yield 92%). <sup>1</sup>H NMR (500 MHz, DMSO-*d*<sub>6</sub>) δ 13.25 (s, 1H), 11.11 (s, 1H), 7.79 (dd, *J* = 8.5, 7.3 Hz, 1H), 7.47 (d, *J* = 7.2 Hz, 1H), 7.39 (d, *J* = 8.6 Hz, 1H), 5.10 (dd, *J* = 12.8, 5.4 Hz, 1H), 4.98 (s, 2H), 2.93–2.85 (m, 1H), 2.63–2.51 (m, 2H), 2.08–2.00 (m, 1H). HRMS (ESI)  $m/z$ : calcd C<sub>15</sub>H<sub>13</sub>N<sub>2</sub>O<sub>7</sub><sup>+</sup>  $[M+H]^+$ , 333.0717; found, 333.0719.

4.1.26. *N*-(2-chloro-6-methylphenyl)-2-((6-(4-(2-((2-(2,6-dioxopiperidin-3-yl)-1,3-dioxoisindolin-4-yl)oxy)acetyl)piperazin-1-yl)-2-methylpyrimidin-4-yl)amino)thiazole-5-carboxamide (**14**)

The derivative **14** was obtained from the condensation of **S16** and **S2** according the similar process of **4**. Yellow solid, 18.5 mg, (yield 52%). <sup>1</sup>H NMR (500 MHz, CD<sub>3</sub>OD) δ 8.21 (s, 1H), 7.77 (dd, *J* = 8.5, 7.3 Hz, 1H), 7.51 (d, *J* = 7.1 Hz, 1H), 7.42 (d, *J* = 8.5 Hz, 1H), 7.36 (dd, *J* = 7.2, 1.9 Hz, 1H), 7.28–7.22 (m, 2H), 6.30 (s, 1H), 5.17 (d, *J* = 2.3 Hz, 2H), 5.14–5.08 (m, 1H), 3.80 (d, *J* = 29.3 Hz, 8H), 2.90–2.80 (m, 1H), 2.78–2.68 (m, 2H), 2.61 (s, 3H), 2.31 (s, 3H), 2.16–2.10 (m, 1H). <sup>13</sup>C NMR (126 MHz, DMSO-*d*<sub>6</sub>) δ 172.80, 169.95, 166.81, 165.37, 165.28, 160.73, 159.61, 156.67, 155.59, 138.79, 136.57, 133.41, 133.10, 132.42, 129.05, 128.24, 127.03, 120.26, 116.16, 115.51, 109.53, 83.40, 76.61, 66.10, 48.77, 43.94, 43.75, 43.18, 40.71, 30.96, 22.00, 18.32. HRMS (ESI)  $m/z$ : calcd C<sub>35</sub>H<sub>33</sub>ClN<sub>9</sub>O<sub>7</sub>S<sup>+</sup>  $[M+H]^+$ , 758.1907; found, 758.1913.

4.1.27. 4-bromo-2-(2,6-dioxopiperidin-3-yl)isoindoline-1,3-dione (**S18**)

4-bromoisobenzofuran-1,3-dione **S17** (500 mg, 2.20 mmol), 3-aminoperidol 2,6-dione (400 mg, 2.42 mmol) and anhydrous sodium acetate (220 mg, 2.64 mmol) were added to a 100 ml egg-like bottle, followed by glacial acetic acid (10 ml). The reaction solution was then slowly raised to 140 °C and stirred for 12 h. After the reaction was finished, the reaction liquid was reduced to room temperature and a large amount of white solid was precipitated. After filtrated the solvent, the solid was washed with the mixture of water (10 mL) and methanol (2 mL) fully stirred for 0.5 h. then filtration, the filter cake was washed with water to afford drying compound **S18**, white solid, 700 mg, (yield 94%). <sup>1</sup>H NMR (500 MHz, DMSO-*d*<sub>6</sub>) δ 11.14 (s, 1H), 8.14 (d, *J* = 1.4 Hz, 1H), 8.09 (dd, *J* = 7.9, 1.7 Hz, 1H), 7.86 (d, *J* = 7.9 Hz, 1H), 5.16 (dd, *J* = 12.9, 5.4 Hz, 1H), 2.93–2.85 (m, 1H), 2.65–2.50 (m, 2H), 2.08–2.04 (m, 1H). HRMS (ESI)  $m/z$ : calcd C<sub>13</sub>H<sub>10</sub>BrN<sub>2</sub>O<sub>4</sub><sup>+</sup>  $[M+H]^+$ , 336.9818; found, 336.9810.

4.1.28. *tert*-butyl (*E*)-3-(2-(2,6-dioxopiperidin-3-yl)-1,3-dioxoisindolin-4-yl)acrylate (**S19**)

*Tert*-butylphosphine tetrafluoroboric acid (110 mg,

0.38 mmol), *n*-methyl dicyclohexylamine (250 mg, 1.28 mmol), Pd<sub>2</sub>(dba)<sub>3</sub> (163 mg, 0.64 mmol) and anhydrous dioxane (6 ml) were added to a 50 ml egg-shaped bottle and stirred at room temperature for 30 min. The compound **S18** (300 mg, 0.89 mmol) and *tert*-butyl acrylate (228 mg, 1.98 mmol) were then added. After that, the reaction liquid was slowly raised to 55 °C under nitrogen protection and stirred for 12 h. Then the reaction solvent was steamed by decompression, the silica gel sample was mixed, and the compound **S19** was purified by column chromatography (eluent: 40% EA/PE). Yellow solid, 270 mg, (yield 79%). <sup>1</sup>H NMR (500 MHz, CDCl<sub>3</sub>) δ 8.11 (s, 1H), 8.02 (s, 1H), 7.89 (d, *J* = 7.7 Hz, 1H), 7.84 (dd, *J* = 7.8, 1.2 Hz, 1H), 7.65 (d, *J* = 16.0 Hz, 1H), 6.54 (d, *J* = 16.0 Hz, 1H), 5.00 (dd, *J* = 12.5, 5.3 Hz, 1H), 2.94–2.72 (m, 3H), 2.20–2.13 (m, 1H), 1.54 (s, 9H). HRMS (ESI)  $m/z$ : calcd C<sub>20</sub>H<sub>21</sub>N<sub>2</sub>O<sub>6</sub><sup>+</sup>  $[M+H]^+$ , 385.1394; found, 385.1389.

4.1.29. 3-(2-(2,6-dioxopiperidin-3-yl)-1,3-dioxoisindolin-4-yl)propanoic acid (**S20**)

The compound **S19** (250 mg, 0.65 mmol) was added to a 100 ml egg-shaped bottle, followed by dioxide-hexacyclic (20 ml) and 10% wet Pd/C, respectively. The reaction system was replaced with H<sub>2</sub> (25 psi) for three times, and the reaction liquid was stirred overnight at room temperature. After that, the filtrate was extracted and washed with the dioxy-hexane ring. The filtrate was concentrated under decompression to produce a yellowish oily substance. The crude product was not further purified and was directly used in the next step of reaction. The obtained crude, TFA (1 ml) and anhydrous dichloromethane (5 ml) were added to a 50 ml egg-shaped bottle, and then stirred at room temperature for 2 h. After the reaction was complete, the reaction solvent was removed by decompression, and the crude product was prepared in a reversed phase column of C18 to afford compound **S20** after freeze-drying. White solid, 180 mg, (two-step, yield 84%). <sup>1</sup>H NMR (500 MHz, DMSO-*d*<sub>6</sub>) δ 12.22 (s, 1H), 11.12 (s, 1H), 7.86–7.79 (m, 2H), 7.77–7.70 (m, 1H), 5.13 (dd, *J* = 12.8, 5.4 Hz, 1H), 3.01 (t, *J* = 7.4 Hz, 2H), 2.93–2.85 (m, 1H), 2.64 (t, *J* = 7.4 Hz, 2H), 2.62–2.50 (m, 2H), 2.08–2.02 (m, 1H). HRMS (ESI)  $m/z$ : calcd C<sub>16</sub>H<sub>15</sub>N<sub>2</sub>O<sub>6</sub><sup>+</sup>  $[M+H]^+$ , 331.0925; found, 331.0919.

4.1.30. *N*-(2-chloro-6-methylphenyl)-2-((6-(4-(3-(2-(2,6-dioxopiperidin-3-yl)-1,3-dioxoisindolin-4-yl)propanoyl)piperazin-1-yl)-2-methylpyrimidin-4-yl)amino)thiazole-5-carboxamide (**15**)

The derivative **15** was obtained from the condensation of **S20** and **S2** according the similar process of **4**. White solid, 24.2 mg, (yield 47%). <sup>1</sup>H NMR (500 MHz, DMSO-*d*<sub>6</sub>) δ 11.12 (s, 1H), 9.94 (s, 1H), 8.25 (s, 1H), 7.88–7.82 (m, 2H), 7.78 (dd, *J* = 7.8, 1.1 Hz, 1H), 7.40 (d, *J* = 7.7 Hz, 1H), 7.31–7.23 (m, 2H), 6.12 (s, 1H), 5.14 (dd, *J* = 12.8, 5.4 Hz, 1H), 3.59 (s, 6H), 3.49 (dd, *J* = 7.8, 3.0 Hz, 1H), 3.41 (dd, *J* = 7.8, 3.0 Hz, 1H), 3.04 (t, *J* = 7.5 Hz, 2H), 2.93–2.85 (m, 1H), 2.80 (t, *J* = 7.5 Hz, 2H), 2.64–2.52 (m, 2H), 2.45 (s, 3H), 2.24 (s, 3H), 2.06–2.02 (m, 1H). <sup>13</sup>C NMR (126 MHz, DMSO-*d*<sub>6</sub>) δ 172.79, 172.69, 169.88 (d, *J* = 8.7 Hz), 167.33, 167.14, 159.61, 156.58, 149.78, 149.11, 138.80, 135.04, 133.41, 132.43, 131.57 (d, *J* = 7.2 Hz), 129.05, 128.25, 127.04, 123.61, 123.36, 83.36, 72.28, 48.97, 44.02 (d, *J* = 39.0 Hz), 40.45, 34.62, 33.37, 30.96, 30.64, 22.04, 18.32. HRMS (ESI)  $m/z$ : calcd C<sub>36</sub>H<sub>35</sub>ClN<sub>9</sub>O<sub>6</sub>S<sup>+</sup>  $[M+H]^+$ , 756.2114; found, 756.2114.

4.1.31. *tert*-butyl 2-((2-(2,6-dioxopiperidin-3-yl)-1,3-dioxoisindolin-4-yl)sulfonyl)acetate (**S11**)

The compound **S9** (0.45 g, 1.1 mmol) was added to a 100 ml egg-shaped bottle, followed by an anhydrous DCM (20 ml), and then slowly added to *m*-CPBA (0.76 g, 4.4 mmol) after stirring at 40 °C for 4 h. After the reaction was completed, the reaction mixture cooled to room temperature, with 10% NaHCO<sub>3</sub> solution to adjust the pH = 8–9. After that, the mixture was extracted with DCM (2 × 30 ml), organic phase was washed with water (2 × 20 ml) and

saturated salt water (50 ml), then dried with anhydrous Na<sub>2</sub>SO<sub>4</sub>. After removed the solvent, crude products was purified by column chromatography (eluent (v/v): PE/EA = 1:1) to afford compound **S11**, light yellow solid, 0.3 g, (yield 59%). <sup>1</sup>H NMR (500 MHz, CDCl<sub>3</sub>) δ 8.42 (dd, *J* = 7.9, 0.9 Hz, 1H), 8.19 (dd, *J* = 7.5, 0.9 Hz, 1H), 8.12 (s, 1H), 8.00 (t, *J* = 7.7 Hz, 1H), 5.03 (dd, *J* = 12.6, 5.4 Hz, 1H), 4.72–4.64 (m, 2H), 2.96–2.72 (m, 3H), 2.26–2.17 (m, 1H), 1.30 (s, 9H). MS (ESI, *m/z*): 437 [M+H]<sup>+</sup>.

#### 4.1.32. 2-((2-(2,6-dioxopiperidin-3-yl)-1,3-dioxoisindolin-4-yl)sulfonyl)acetic acid (**S12**)

The synthesis of intermediate **S12** was similar to **S10**. Yellow solid, 0.25 g, (yield 96%). <sup>1</sup>H NMR (500 MHz, DMSO-*d*<sub>6</sub>) δ 11.20 (s, 1H), 8.35–8.25 (m, 2H), 8.14 (t, *J* = 7.7 Hz, 1H), 5.23 (dd, *J* = 12.9, 5.4 Hz, 1H), 4.96–4.73 (m, 2H), 2.93–2.86 (m, 1H), 2.66–2.51 (m, 2H), 2.13–2.08 (m, 1H). MS (ESI, *m/z*): 381 [M+H]<sup>+</sup>.

#### 4.1.33. *N*-(2-chloro-6-methylphenyl)-2-((6-(4-(2-((2,6-dioxopiperidin-3-yl)-1,3-dioxoisindolin-4-yl)sulfonyl)acetyl)piperazin-1-yl)-2-methylpyrimidin-4-yl)amino)thiazole-5-carboxamide (**16**)

The derivative **16** was obtained from the condensation of **S12** and **S2** according the similar process of **12**. Yellow solid, 25.2 mg, (yield 69%). <sup>1</sup>H NMR (500 MHz, CD<sub>3</sub>OD) δ 8.38 (dd, *J* = 7.9, 0.9 Hz, 1H), 8.25 (dd, *J* = 7.5, 0.9 Hz, 1H), 8.20 (s, 1H), 8.09 (t, *J* = 7.7 Hz, 1H), 7.37 (dd, *J* = 7.4, 1.8 Hz, 1H), 7.31–7.19 (m, 2H), 6.24 (s, 1H), 5.25 (dd, *J* = 12.6, 5.5 Hz, 1H), 5.06 (dd, *J* = 22.0, 14.0 Hz, 2H), 3.95–3.86 (m, 4H), 3.80–3.66 (m, 4H), 2.94–2.85 (m, 1H), 2.82–2.70 (m, 2H), 2.58 (s, 3H), 2.32 (s, 3H), 2.25–2.16 (m, 1H). <sup>13</sup>C NMR (126 MHz, DMSO-*d*<sub>6</sub>) δ 172.73, 169.50, 165.71, 164.61, 162.04, 160.07, 159.88, 158.20 (d, *J* = 36.5 Hz), 156.97, 140.76, 138.82, 137.03, 135.73, 134.26, 133.50, 133.15, 132.43, 129.05, 128.25, 128.10, 127.02, 125.90, 82.95, 57.36, 49.39, 45.22, 43.59, 42.96, 41.20, 30.89, 25.48, 21.84, 18.30. MS (ESI, *m/z*): 806 [M+H]<sup>+</sup>.

#### 4.1.34. 1-(2-chloroethyl)piperazine (**S22**)

SOCl<sub>2</sub> (10 mL) was added to a 100 ml single-mouth bottle, followed by a slow addition of the compound 1-(2-hydroxyethyl)piperazine **S21** (800 mg, 6.14 mmol), followed by reflux agitation for 12 h. The reaction liquid was cooled to room temperature. After removed the solvent, a large number of grey-yellow solids were precipitated, then water was added, and the crude product was freeze-dried. The crude product **S22** was not purified and was directly used in the next step of the reaction, 810 mg, (yield 89%). <sup>1</sup>H NMR (500 MHz, DMSO-*d*<sub>6</sub>) δ 9.65 (s, 1H), 4.39–3.14 (m, 12H).

#### 4.1.35. *N*-(2-chloro-6-methylphenyl)-2-((6-(4-(2-chloroethyl)piperazin-1-yl)-2-methylpyrimidin-4-yl)amino)thiazole-5-carboxamide (**S23**)

The compound **S2** (100 mg, 0.25 mmol), **S22** (145 mg, 1.00 mmol) and *N,N*-diisopropyl ethylamine (130 mg, 1.00 mmol) were added to a 50 ml egg-shaped bottle, followed by an anhydrous DMF (3 ml), which was then slowly heated to 110 °C under nitrogen protection and stirred overnight. Then reaction liquid was cooled to room temperature, then pour into 50 ml of water, and extracted with EA (2 × 50 ml), organic phase was washed with water (3 × 20 ml) and saturated salt water (20 ml), dried with anhydrous Na<sub>2</sub>SO<sub>4</sub> then removed solvent, the crude products was purified by column chromatography (eluent (v/v), DCM/MeOH = 20:1) to afford product **S23**. White solid, 50 mg, (yield 39%). <sup>1</sup>H NMR (500 MHz, DMSO-*d*<sub>6</sub>) δ 11.47 (s, 1H), 9.87 (s, 1H), 8.22 (s, 1H), 7.40 (d, *J* = 6.6 Hz, 1H), 7.30–7.23 (m, 2H), 6.06 (s, 1H), 3.72 (t, *J* = 6.4 Hz, 2H), 3.57–3.47 (m, 4H), 2.69 (t, *J* = 6.3 Hz, 2H), 2.51–2.55 (m, 4H), 2.41 (s, 3H), 2.24 (s, 3H). MS (ESI, *m/z*): 505 [M+H]<sup>+</sup>.

#### 4.1.36. *N*-(2-chloro-6-methylphenyl)-2-((6-(4-(2-((2,6-dioxopiperidin-3-yl)-1,3-dioxoisindolin-4-yl)thio)ethyl)piperazin-1-yl)-2-methylpyrimidin-4-yl)amino)thiazole-5-carboxamide (**17**)

The compounds **S23** (20 mg, 0.04 mmol), **S8** (13 mg, 0.044 mmol), anhydrous K<sub>2</sub>CO<sub>3</sub> (27.6 mg, 0.2 mmol) and NaI (30 mg, 0.2 mmol) were added to a 10 ml egg-shaped bottle, followed by adding anhydrous DMF (3 mL), slowly rising to 60 °C and stirring for 8 h. After the reaction was completed, the reaction mixture was filtered, and the filtrate was prepared and separated by HPLC to obtain the target compound **17**. White solid, 20.2 mg, (yield 68%). <sup>1</sup>H NMR (500 MHz, DMSO-*d*<sub>6</sub>) δ 11.50 (s, 1H), 11.13 (s, 1H), 9.93 (s, 1H), 8.26 (s, 1H), 7.97 (d, *J* = 8.3 Hz, 1H), 7.84 (t, *J* = 7.7 Hz, 1H), 7.71 (d, *J* = 7.3 Hz, 1H), 7.40 (d, *J* = 7.6 Hz, 1H), 7.32–7.23 (m, 2H), 6.18 (s, 1H), 5.13 (dd, *J* = 12.9, 5.4 Hz, 1H), 4.39–4.37 (m, 2H), 3.73–3.66 (m, 4H), 3.44–3.35 (m, 4H), 3.18–3.07 (m, 2H), 2.93–2.85 (m, 1H), 2.64–2.52 (m, 2H), 2.46 (s, 3H), 2.24 (s, 3H), 2.08–2.01 (m, 1H). <sup>13</sup>C NMR (126 MHz, DMSO-*d*<sub>6</sub>) δ 173.27, 170.38, 167.17, 165.68, 163.05, 162.77, 160.42, 157.42, 141.32, 139.41, 139.30, 135.43, 134.00, 132.94, 130.89, 129.50, 128.64, 127.48, 126.19, 125.90, 119.34, 83.14, 56.42, 52.45, 49.38, 43.99, 31.44, 27.74, 26.06, 22.45, 18.79. MS (ESI, *m/z*): 760 [M+H]<sup>+</sup>. HRMS (ESI) *m/z*: calcd C<sub>35</sub>H<sub>35</sub>ClN<sub>9</sub>O<sub>5</sub>S<sub>2</sub><sup>+</sup> [M+H]<sup>+</sup>, 760.1886; found, 760.1881.

#### 4.1.37. 3-(4-(benzylthio)-1-oxoisindolin-2-yl)piperidine-2,6-dione (**S26**)

Na<sub>2</sub>S<sub>2</sub>O<sub>3</sub>·5H<sub>2</sub>O (53.7 g, 216.3 mmol), BnCl (27.4 g, 216.3 mmol), CuSO<sub>4</sub>·5H<sub>2</sub>O (77.4 mg, 0.31 mmol) and 2,2'-bipyridine (0.72 g, 4.6 mmol) were added to a 500 ml egg-shaped bottle containing methanol (120 ml) and water (120 ml), and then slowly heated to 80 °C and stirred for 2 h. The reaction solution was then brought to room temperature, lenalidomide **S25** (8.0 g, 30.9 mmol) was added, and *tert*-butylnitrite (4.78 g, 46.4 mmol) was slowly added. The solution was then raised again to 80 °C and stirred for 8 h. After the reaction was completed, the reaction liquid was reduced to room temperature, water (200 ml) was added, extracted with EA (2 × 200 mL), washed (2 × 50 mL) with saturated salt (50 ml), Then the solvent was evaporated, and the crude was purified by column chromatography (eluent (v/v): PE/EA = 1:2) to obtain the target compound **S26**. White solid, 6.8 g, (yield 60%). <sup>1</sup>H NMR (500 MHz, CDCl<sub>3</sub>) δ 8.07 (s, 1H), 7.75 (t, *J* = 7.3 Hz, 1H), 7.55 (dd, *J* = 7.4, 6.8 Hz, 1H), 7.49–7.41 (m, 1H), 7.27–7.17 (m, 5H), 5.20–5.17 (m, 1H), 4.22 (d, *J* = 16.5 Hz, 1H), 4.15–4.04 (m, 2H), 3.92 (d, *J* = 16.5 Hz, 1H), 2.95–2.74 (m, 2H), 2.32–2.22 (m, 1H), 2.17–2.11 (m, 1H). MS (ESI, *m/z*): 367 [M+H]<sup>+</sup>.

#### 4.1.38. 3-(4-mercapto-1-oxoisindolin-2-yl)piperidine-2,6-dione (**S24**)

Anhydrous AlCl<sub>3</sub> (2.61 g, 19.6 mmol) and anhydrous toluene (70 ml) were added to a 250 ml egg-shaped bottle, and slowly added **S26** (1.8 g, 4.9 mmol) after agitation. After the reaction was completed, 20% citric acid solution was added slowly under agitation, and a large amount of solid was precipitated. After filtration, the precipitate was washed with water and EA respectively, and was dried to obtain the target compound **S24**, white solid, 1.15 g, (yield 85%). <sup>1</sup>H NMR (500 MHz, DMSO-*d*<sub>6</sub>) δ 11.01 (s, 1H), 7.82–7.39 (m, 3H), 5.73 (s, 1H), 5.21–5.04 (m, 1H), 4.40–4.20 (m, 2H), 2.99–2.85 (m, 1H), 2.67–2.56 (m, 1H), 2.47–2.30 (m, 1H), 2.05–1.95 (m, 1H). MS (ESI, *m/z*): 276 [M+H]<sup>+</sup>.

#### 4.1.39. 2-((2-(2,6-dioxopiperidin-3-yl)-1-oxoisindolin-4-yl)thio)acetic acid (**S27**)

The synthesis of intermediate **S27** was similar to **S10**. white solid, 1.2 g, (65% yield over two steps) <sup>1</sup>H NMR (500 MHz, DMSO-*d*<sub>6</sub>) δ 12.88 (s, 1H), 11.00 (s, 1H), 7.68–7.45 (m, 3H), 5.15–5.13 (m, 1H), 4.32 (dd, *J* = 56.2, 17.3 Hz, 2H), 3.94 (s, 2H), 2.95–2.91 (m, 1H),

2.63–2.59 (m, 1H), 2.49–2.39 (m, 1H), 2.08–1.92 (m, 1H).  $^{13}\text{C}$  NMR (126 MHz, DMSO- $d_6$ )  $\delta$  172.89, 170.95, 170.29, 167.70, 141.11, 132.06, 131.15, 130.92, 129.20, 120.81, 51.66, 46.66, 34.45, 31.22, 22.36. MS (ESI,  $m/z$ ): 334  $[\text{M}+\text{H}]^+$ .

4.1.40. *N*-(2-chloro-6-methylphenyl)-2-((6-(4-(2-((2-(2,6-dioxopiperidin-3-yl)-1-oxoisindolin-4-yl)thio)acetyl)piperazin-1-yl)-2-methylpyrimidin-4-yl)amino)thiazole-5-carboxamide (**18**)

The derivative **18** was obtained from the condensation of **S27** and **S2** according to the similar process of **12**. White solid, 10 mg, (yield 39%).  $^1\text{H}$  NMR (500 MHz, DMSO- $d_6$ )  $\delta$  11.55 (s, 1H), 10.99 (s, 1H), 9.90 (s, 1H), 8.23 (s, 1H), 7.76–7.71 (m, 1H), 7.60 (d,  $J = 6.8$  Hz, 1H), 7.53 (t,  $J = 7.6$  Hz, 1H), 7.40 (d,  $J = 6.4$  Hz, 1H), 7.32–7.18 (m, 2H), 6.09 (s, 1H), 5.13 (dd,  $J = 13.3, 5.1$  Hz, 1H), 4.42 (d,  $J = 17.4$  Hz, 1H), 4.28 (d,  $J = 17.4$  Hz, 1H), 4.20 (s, 2H), 3.66–3.52 (m, 10H), 2.95–2.85 (m, 1H), 2.64–2.57 (m, 1H), 2.45 (d,  $J = 13.0$  Hz, 5H), 2.24 (s, 3H), 2.04–1.94 (m, 1H).  $^{13}\text{C}$  NMR (126 MHz, DMSO- $d_6$ )  $\delta$  172.89, 170.98, 167.77, 166.23, 164.28, 162.54, 161.59, 159.83, 156.88, 141.49, 140.88, 138.82, 133.48, 132.43, 131.95 (d,  $J = 8.1$  Hz), 131.22, 129.10 (d,  $J = 10.8$  Hz), 128.23, 127.03, 125.98, 120.86, 83.05, 51.67, 46.75, 44.67, 43.72, 43.30, 41.03, 35.25, 31.23, 25.19, 22.38, 18.31. MS (ESI,  $m/z$ ): 760  $[\text{M}+\text{H}]^+$ .

4.1.41. *N*-(2-chloro-6-methylphenyl)-2-((6-(4-(2-((2-(2,6-dioxopiperidin-3-yl)-1-oxoisindolin-4-yl)thio)ethyl)piperazin-1-yl)-2-methylpyrimidin-4-yl)amino)thiazole-5-carboxamide (**19**)

The derivative **19** was obtained from the condensation of **S23** and **S24** according to the similar process of **17**. White solid, 6.0 mg, (yield 27%).  $^1\text{H}$  NMR (500 MHz, CD $_3$ OD)  $\delta$  8.22 (s, 1H), 7.79 (ddd,  $J = 24.9, 11.2, 3.9$  Hz, 2H), 7.60 (dd,  $J = 17.9, 10.2$  Hz, 1H), 7.36 (dd,  $J = 7.2, 2.0$  Hz, 1H), 7.32–7.15 (m, 2H), 6.42 (d,  $J = 29.7$  Hz, 1H), 5.18 (dd,  $J = 13.3, 5.2$  Hz, 1H), 4.58–4.46 (m, 2H), 4.18–3.31 (m, 12H), 2.95–2.88 (m, 1H), 2.79 (ddd,  $J = 17.5, 4.5, 2.3$  Hz, 1H), 2.64–2.46 (m, 4H), 2.31 (s, 3H), 2.19 (ddd,  $J = 10.4, 5.2, 2.6$  Hz, 1H).  $^{13}\text{C}$  NMR (126 MHz, DMSO- $d_6$ )  $\delta$  172.90, 170.97, 167.65, 165.12, 161.53, 159.78, 157.18, 141.55, 138.82, 133.48, 132.42 (d,  $J = 6.1$  Hz), 130.88, 129.65, 129.49, 129.06, 128.24, 127.04, 126.07, 121.16, 83.70, 66.46, 61.23, 54.12, 51.70, 50.00, 46.75, 40.94, 31.22, 24.89, 22.40, 18.33. MS (ESI,  $m/z$ ): 746  $[\text{M}+\text{H}]^+$ .

4.1.42. *tert*-butyl (4-(4-(6-((5-((2-chloro-6-methylphenyl) carbamoyl)thiazol-2-yl)amino)-2-methyl pyrimidin-4-yl)piperazin-1-yl)butyl)carbamate (**S28**)

The compound **S2** (200 mg, 0.45 mmol) was added to a 25 ml egg-shaped bottle, followed by anhydrous DMF (5 ml), anhydrous K $_2$ CO $_3$  (125 mg, 0.90 mmol) and NaI (135 mg, 0.90 mmol), stirred at room temperature and then added to *tert*-butyl (4-bromobutyl) carbamate (227 mg, 0.90 mmol), slowly heated to 110 °C and stirred overnight. After the reaction was completed, 30 ml of water was poured into the reaction mixture, extracted with EA (2  $\times$  30 ml), organic phase was washed with water (3  $\times$  10 ml) and saturated salt (10 ml), dried with anhydrous Na $_2$ SO $_4$ , then the solvent was evaporated, the crude was purified by column chromatography (eluent (v/v): DCM/MeOH = 10:1) to afford compound **S28**, white solid, 110 mg, (yield 52%).  $^1\text{H}$  NMR (500 MHz, DMSO- $d_6$ )  $\delta$  11.46 (s, 1H), 9.87 (s, 1H), 8.22 (s, 1H), 7.40 (d,  $J = 6.5$  Hz, 1H), 7.31–7.23 (m, 2H), 6.85–6.80 (m, 1H), 6.05 (s, 1H), 3.54–3.47 (m, 4H), 2.98–2.84 (m, 4H), 2.40 (s, 3H), 2.41–2.38 (m, 2H), 2.30–2.26 (m, 2H), 2.24 (s, 3H), 1.44–1.38 (m, 4H), 1.37 (s, 9H). MS (ESI,  $m/z$ ): 615  $[\text{M}+\text{H}]^+$ .

4.1.43. *N*-(2-chloro-6-methylphenyl)-2-((6-(4-(4-((2-(2,6-dioxopiperidin-3-yl)-1,3-dioxoisindolin-4-yl)amino)butyl)piperazin-1-yl)-2-methylpyrimidin-4-yl)amino)thiazole-5-carboxamide (**20**)

The compound **S28** (110 mg, 0.18 mmol) was added to a 25 ml

egg-shaped bottle, followed by anhydrite DCM (1 ml) and TFA (3 ml), and stirred at room temperature for 2 h. Then evaporated the solvent and added the mixture of DCM/MeOH (10:1, ml), and adjusted the pH to 8–9 with saturated NaHCO $_3$  solution and extracted with 10% of the DCM/methanol solution (2  $\times$  11 ml). Organic phase was washed with saturated salt water (10 ml), dried with anhydrous Na $_2$ SO $_4$ . After removed the solvent, the obtained white solid (90 mg) was used for the next step without further purification.

The obtained crude compound (15 mg, 0.03 mmol), **S3** (8 mg, 0.03 mmol) and DIPEA (37 mg, 0.3 mmol) were added to a 25 ml egg-like bottle, followed by NMP (5 ml), which was slowly raised to 110 °C and stirred for 12 h. After that, the reaction solution was reduced to room temperature, poured into 50% salt water (30 ml), extracted with EA (3  $\times$  30 ml), and washed with water (2  $\times$  20 ml), saturated salt (20 ml), dried with anhydrous Na $_2$ SO $_4$ . After removed the solvent, the crude product was prepared and separated by HPLC to obtained the final compound **20**, yellow solid, 6.3 mg, (yield 28%).  $^1\text{H}$  NMR (500 MHz, CD $_3$ OD)  $\delta$  8.26 (s, 1H), 8.01 (s, 3H), 7.58 (dd,  $J = 8.5, 7.1$  Hz, 1H), 7.37 (dd,  $J = 7.1, 2.2$  Hz, 1H), 7.28–7.24 (m, 2H), 7.12 (d,  $J = 8.6$  Hz, 1H), 7.07 (d,  $J = 7.1$  Hz, 1H), 6.53 (s, 1H), 5.06 (dd,  $J = 12.4, 5.5$  Hz, 1H), 4.82–4.58 (m, 2H), 3.75 (d,  $J = 12.1$  Hz, 2H), 3.67–3.60 (m, 2H), 3.46 (t,  $J = 6.6$  Hz, 2H), 3.30–3.19 (m, 4H), 2.86–2.80 (m, 1H), 2.76–2.69 (m, 2H), 2.66 (s, 3H), 2.32 (s, 3H), 2.14–2.08 (m, 1H), 1.98–2.00 (m, 2H), 1.81–1.74 (m, 2H). MS (ESI,  $m/z$ ): 771  $[\text{M}+\text{H}]^+$ .

4.1.44. 5-bromo-*N*-(2-(2,6-dioxopiperidin-3-yl)-1,3-dioxoisindolin-4-yl)pentanamide (**S30**)

The compound pomalidomide **S29** (500 mg, 1.83 mmol) and anhydrous THF (15 ml) were added to a 100 ml egg-shaped bottle, stirred at room temperature and slowly added with 5-bromopentanoyl chloride (1.83 g, 9.15 mmol), then slowly warmed to reflux and stir for 3 h. After the reaction was completed, the reaction liquid was cooled to room temperature, and 3 ml of methanol was added to quench and stirred for 30 min. Then the reaction solvent was removed to obtain the solid crude product. The solid was then beaten with 10 mL (EA/PE = 10:1), filtered and washed to produce a pale yellow solid **S30**. Pale yellow solid, 750 mg, (yield 94%).  $^1\text{H}$  NMR (500 MHz, DMSO- $d_6$ )  $\delta$  11.14 (s, 1H), 9.73 (s, 1H), 8.45 (d,  $J = 8.3$  Hz, 1H), 7.88–7.76 (m, 1H), 7.68–7.57 (m, 1H), 5.14 (dd,  $J = 12.9, 5.4$  Hz, 1H), 3.58 (t,  $J = 6.6$  Hz, 2H), 2.93–2.86 (m, 1H), 2.65–2.57 (m, 1H), 2.56–2.51 (m, 2H), 2.08–2.04 (m, 1H), 1.91–1.85 (m, 2H), 1.80–1.69 (m, 2H). MS (ESI,  $m/z$ ): 436  $[\text{M}+\text{H}]^+$ .

4.1.45. *N*-(2-chloro-6-methylphenyl)-2-((6-(4-(5-((2-(2,6-dioxopiperidin-3-yl)-1,3-dioxoisindolin-4-yl)amino)-5-oxopentyl)piperazin-1-yl)-2-methylpyrimidin-4-yl)amino)thiazole-5-carboxamide (**21**)

The compound **S2** (20 mg, 0.045 mmol) was added to a 25 ml egg-shaped bottle, followed by anhydric DMF (2 ml), DIPEA (30 mg, 0.225 mmol) and NaI (13.5 mg, 0.09 mmol). Then **S30** (39 mg, 0.09 mmol) was added and stirred at room temperature. After the reaction was completed by LC-MS detection, the reaction liquid was filtered, and the filtrate was prepared and separated by HPLC to obtained **21** after freeze-drying. White solid, 10.8 mg, (yield 29%).  $^1\text{H}$  NMR (500 MHz, CD $_3$ OD)  $\delta$  8.59 (d,  $J = 8.4$  Hz, 1H), 8.21 (s, 1H), 7.83–7.78 (m, 1H), 7.62 (d,  $J = 7.1$  Hz, 1H), 7.37 (d,  $J = 5.6$  Hz, 1H), 7.28–7.23 (m, 2H), 6.33 (s, 1H), 5.15 (dd,  $J = 12.7, 5.5$  Hz, 1H), 3.75–3.72 (m, 2H), 3.50–3.40 (m, 2H), 3.35–3.27 (m, 4H), 3.23–3.17 (m, 2H), 2.89–2.84 (m, 1H), 2.79–2.69 (m, 2H), 2.64 (t,  $J = 6.9$  Hz, 2H), 2.58 (s, 3H), 2.32 (s, 3H), 2.19–2.15 (m, 1H), 1.97–1.90 (m, 2H), 1.88–1.82 (m, 2H).  $^{13}\text{C}$  NMR (126 MHz, DMSO- $d_6$ )  $\delta$  172.79, 171.53, 169.81, 167.60, 166.67, 165.13, 162.36, 161.65, 159.81, 157.17, 138.81, 136.39, 136.11, 133.49, 132.44, 131.52, 129.05, 128.21, 127.03,

126.64, 126.07, 123.75, 118.51, 117.35, 83.58, 55.12, 50.13, 48.93, 40.79, 35.63, 30.95, 25.33, 22.54, 22.01, 21.83, 18.32. MS (ESI,  $m/z$ ): 799  $[M+H]^+$ .

4.1.46. 5-((2-(2,6-dioxopiperidin-3-yl)-1-oxoisindolin-4-yl)amino)pentanoic acid (**S33**)

The compound lenalidomide **S31** (259.3 mg, 1 mmol) was added to a 25 ml egg-like bottle, followed by anhydrous NMP (5 ml), *N,N*-diisopropyl ethylamine (387.7 mg, 3 mmol) and *tert*-butyl bromopentate (284.6 mg, 1.2 mmol). The solution was then added, slowly raised to 100 °C and stirred overnight. After that, the reaction was purified by C18 reverse phase column to afford target compound **S32** with a pale yellow solid, 260 mg, (yield 63%).

The obtained intermediate **S32** (260 mg, 0.62 mmol), TFA (2 mL) and anhydrous dichloromethane (10 mL) were added to a 50 mL egg-shaped bottle and stirred for 2 h at room temperature. After that, the reaction solvent was removed by decompression, and the crude product was prepared by C18 reversed phase column to afford compound (**S33**) with a white solid, 210 mg, (yield 93%). <sup>1</sup>H NMR (500 MHz, DMSO-*d*<sub>6</sub>) δ 11.00 (s, 1H), 7.28 (t, *J* = 7.7 Hz, 1H), 6.92 (t, *J* = 10.9 Hz, 1H), 6.76 (d, *J* = 8.0 Hz, 1H), 5.11 (dd, *J* = 13.3, 5.1 Hz, 1H), 5.07–4.83 (m, 3H), 4.23 (d, *J* = 17.2 Hz, 1H), 4.13 (d, *J* = 17.1 Hz, 1H), 3.13 (d, *J* = 6.4 Hz, 2H), 2.97–2.87 (m, 1H), 2.61 (d, *J* = 16.7 Hz, 1H), 2.38–2.21 (m, 3H), 2.06–1.98 (m, 1H), 1.67–1.55 (m, 4H). MS (ESI,  $m/z$ ): 360  $[M+H]^+$ .

4.1.47. *N*-(2-chloro-6-methylphenyl)-2-((6-(4-(5-((2-(2,6-dioxopiperidin-3-yl)-1-oxoisindolin-4-yl)amino)pentanoyl)piperazin-1-yl)-2-methylpyrimidin-4-yl)amino)thiazole-5-carboxamide (**22**)

The derivative **22** was obtained from the condensation of **S33** and **S2** according the similar process of **4**. White solid, 10.9 mg, (yield 41%). <sup>1</sup>H NMR (500 MHz, DMSO-*d*<sub>6</sub>) δ 11.63 (s, 1H), 11.00 (s, 1H), 9.93 (s, 1H), 8.25 (s, 1H), 7.40 (d, *J* = 7.9 Hz, 1H), 7.28 (td, *J* = 15.2, 7.4 Hz, 3H), 6.96 (d, *J* = 7.4 Hz, 1H), 6.80 (d, *J* = 8.1 Hz, 1H), 6.12 (s, 1H), 5.11 (dd, *J* = 13.2, 5.3 Hz, 1H), 4.25 (d, *J* = 16.7 Hz, 1H), 4.15 (d, *J* = 17.3 Hz, 1H), 3.59 (s, 8H), 3.16 (s, 2H), 2.92 (t, *J* = 12.8 Hz, 1H), 2.61 (d, *J* = 16.9 Hz, 1H), 2.45 (s, 3H), 2.41 (s, 2H), 2.30 (d, *J* = 8.6 Hz, 1H), 2.24 (s, 3H), 2.04 (s, 1H), 1.63 (s, 4H). MS (ESI,  $m/z$ ): 785  $[M+H]^+$ .

4.1.48. 5-((2-(2,6-dioxopiperidin-3-yl)-1-oxoisindolin-4-yl)amino)-5-oxopentanoic acid (**S34**)

Compound **S31** (4 mmol, 1 equiv) and compound glutaric acid (4 mmol) were added into a dry round-bottom flask. Then HOAt (6 mmol, 1.5 equiv), EDCI (6 mmol, 1.5 equiv), NMM (8 mmol, 2 equiv) and DMF (10 ml) were mixed and stirred at 25 °C for 12 h. The reaction was quenched with water (1.0 ml) followed by purification via preparative HPLC (100 g, C18 column) to afford the desired product **S34**. White solid, 0.52 g, (yield 35%). <sup>1</sup>H NMR (500 MHz, DMSO-*d*<sub>6</sub>) δ 12.09 (s, 1H), 11.01 (s, 1H), 9.80 (s, 1H), 7.81 (dd, *J* = 7.2, 1.8 Hz, 1H), 7.52–7.45 (m, 2H), 5.14 (dd, *J* = 13.3, 5.1 Hz, 1H), 4.40 (d, *J* = 17.5 Hz, 1H), 4.33 (d, *J* = 17.5 Hz, 1H), 2.97–2.87 (m, 1H), 2.64–2.56 (m, 1H), 2.41 (t, *J* = 7.4 Hz, 2H), 2.35 (dd, *J* = 13.1, 4.5 Hz, 1H), 2.29 (t, *J* = 7.3 Hz, 2H), 2.07–1.99 (m, 1H), 1.86–1.78 (m, 2H). MS (ESI,  $m/z$ ): 374  $[M+H]^+$ .

4.1.49. *N*-(2-chloro-6-methylphenyl)-2-((6-(4-(5-((2-(2,6-dioxopiperidin-3-yl)-1-oxoisindolin-4-yl)amino)-5-oxopentanoyl)piperazin-1-yl)-2-methylpyrimidin-4-yl)amino)thiazole-5-carboxamide (**23**)

The derivative **23** was obtained from the condensation of **S34** and **S2** according the similar process of **4**. White solid, 13.1 mg, (yield 49%). <sup>1</sup>H NMR (500 MHz, DMSO-*d*<sub>6</sub>) δ 11.65 (s, 1H), 11.01 (s, 1H), 9.94 (s, 1H), 9.85 (s, 1H), 8.26 (s, 1H), 7.83 (dd, *J* = 7.1,

1.6 Hz, 1H), 7.54–7.46 (m, 2H), 7.40 (d, *J* = 6.4 Hz, 1H), 7.34–7.21 (m, 2H), 6.13 (s, 1H), 5.14 (dd, *J* = 13.3, 5.1 Hz, 1H), 4.38 (dd, *J* = 22.0, 17.5 Hz, 2H), 3.62–3.51 (m, 8H), 2.97–2.86 (m, 1H), 2.63–2.58 (m, 1H), 2.45 (s, 3H), 2.47–2.40 (m, 4H), 2.39–2.30 (m, 1H), 2.24 (s, 3H), 2.06–1.99 (m, 1H), 1.91–1.82 (m, 2H). <sup>13</sup>C NMR (126 MHz, DMSO-*d*<sub>6</sub>) δ 172.90, 171.13 (d, *J* = 9.2 Hz), 170.66, 167.88, 163.68, 162.43, 160.28, 159.57, 156.55, 138.80, 133.79 (d, *J* = 9.1 Hz), 133.39, 132.68, 132.43, 129.08, 128.62, 128.29, 127.06, 125.33, 119.00, 83.46, 51.57, 46.61, 44.15 (d, *J* = 44.9 Hz), 40.36, 35.05, 31.68, 31.23, 24.29, 22.67, 20.63, 18.33. MS (ESI,  $m/z$ ): 799  $[M+H]^+$ .

4.1.50. *N*-(2-chloro-6-methylphenyl)-2-((2-methyl-6-(4-(2-((2-(1-methyl-2,6-dioxopiperidin-3-yl)-1,3-dioxoisindolin-4-yl)thio)ethyl)piperazin-1-yl)pyrimidin-4-yl)amino)thiazole-5-carboxamide (**24**)

To a solution of 2-(2,6-dioxopiperidin-3-yl)-4-fluoroisindoline-1,3-dione (1 g, 3.6 mmol) **S3** in DMF were added K<sub>2</sub>CO<sub>3</sub> (1 g, 7.2 mmol) and MeI (760 mg, 5.4 mmol). After stirring at room temperature for 30 min, the reaction mixture was poured into water and extracted with EtOAc. The combined organic layers were washed with brine, dried over Na<sub>2</sub>SO<sub>4</sub>, and concentrated. The resulting residue was purified by preparative HPLC (10–90% acetonitrile/0.05% HCl in H<sub>2</sub>O) to obtain intermediate (490 mg, 47%) as a white solid. MS (ESI)  $m/z$ : 291. Then the intermediate (100 mg, 0.34 mmol) was dissolved in DMF (150 ml) at room temperature, the Na<sub>2</sub>S<sub>9</sub>H<sub>2</sub>O (125 mg, 0.52 mmol) was added and the mixture were stirred for 3 h under N<sub>2</sub> atmosphere, The reaction was purified by C18 column chromatography (10–90% acetonitrile/0.05% HCl in H<sub>2</sub>O) to obtain **S8-1** faint yellow, 70 mg (yield 68%). MS (ESI)  $m/z$ : 305.

The derivative **24** was obtained from the condensation of **S23** and **S8-1** according the similar process of **17**. White solid, 6.2 mg, (yield 40%). <sup>1</sup>H NMR (500 MHz, DMSO-*d*<sub>6</sub>) δ 11.50 (s, 1H), 9.93 (s, 1H), 8.26 (s, 1H), 7.97 (d, *J* = 8.2 Hz, 1H), 7.84 (t, *J* = 7.7 Hz, 1H), 7.71 (d, *J* = 7.2 Hz, 1H), 7.40 (d, *J* = 7.1 Hz, 1H), 7.33–7.23 (m, 2H), 6.18 (s, 1H), 5.20 (dd, *J* = 13.1, 5.3 Hz, 1H), 4.38 (s, 2H), 3.71–3.63 (m, 4H), 3.42–3.39 (m, 4H), 3.18–3.08 (m, 2H), 3.02 (s, 3H), 2.99–2.90 (m, 1H), 2.80–2.74 (m, 1H), 2.59–2.53 (m, 1H), 2.46 (s, 3H), 2.24 (s, 3H), 2.12–2.04 (m, 1H). <sup>13</sup>C NMR (126 MHz, DMSO-*d*<sub>6</sub>) δ 172.22, 170.10, 167.10 (d, *J* = 9.2 Hz), 165.68, 163.05, 162.78, 160.42, 157.43, 141.32, 139.39 (d, *J* = 21.2 Hz), 135.44, 134.01, 132.94 (d, *J* = 4.8 Hz), 130.91, 129.49, 128.63, 127.48, 126.20, 125.87, 119.34, 83.14, 56.41, 52.45, 49.95, 43.99, 31.58, 27.77, 27.10, 26.06, 21.66, 18.79. HRMS (ESI)  $m/z$ : calcd. C<sub>36</sub>H<sub>37</sub>ClN<sub>9</sub>O<sub>5</sub>S<sub>2</sub><sup>+</sup>  $[M+H]^+$ , 775.3195; found, 775.3191.

## 4.2. Biological screening

### 4.2.1. Cell lines and cell culture

The erythroleukemia cell line K562, derived from a patient in blast crisis CML, and the murine hematopoietic 32D cell was purchased from American Type Culture Collection. All these cells were cultured according to the provider's instructions and maintained at 37 °C in a humidified atmosphere containing 5% CO<sub>2</sub> in air.

### 4.2.2. Cell growth inhibition

For cell growth experiments, 3000 - 20,000 cells/well in 200 μL were seeded into a 96-well tissue culture plate. Then compounds were diluted in the corresponding medium and then 3-fold serially diluted into each well. Cells were incubated for 2 days at 37 °C in an atmosphere of 5% CO<sub>2</sub>. Cell growth was evaluated utilizing CCK-8 assay (CK04, Dojindo Molecular Technologies, MD), incubated for 2–4 h in the cell culture incubator, and read at 450 nm in a microporous plate detection system (PerkinElmer Envision, California). The readings were normalized to the DMSO-treated cells and fitted using a nonlinear regression analysis with the GraphPad

Prism 6 software to obtain the IC<sub>50</sub> value for each compound.

For the establishment of cell lines that exogenously express BCR-ABL proteins, the full-length BCR-ABL cDNA was cloned into plasmid pMIGR1 (Addgen, #27490) and the BCR-ABL mutant isoforms harboring the point mutation G250E, E255K, E255V, F317L, F317V, T315A, and T315I were obtained according to instructions of Stratagene's QuikChange® Lightning Site-Directed Mutagenesis Kit. 32D cells were transduced with retrovirus to express wide-type and mutant isoforms of BCR-ABL and stable transfectants were selected for GFP positive cells by FACS sorting.

#### 4.2.3. Western blotting

$3 \times 10^5$  cells/mL were plated in 24-well plates and treated with compounds at the indicated concentrations and times. Cells were collected, washed with cold  $1 \times$  PBS, and lysed in  $1 \times$  SDS buffer containing protease inhibitor cocktails (no. 539134, Merck). Protein in cell lysate was quantified by detergent compatible Bradford assay kit (no. 23246, Thermo). Primary antibodies used in this study include c-ABL antibody (no. 2862S, Cell Signaling Technology), Phospho-c-ABL (Tyr245) antibody (no. 2861S, Cell Signaling Technology), Stat5 antibody (no. 9363S, Cell Signaling Technology), Phospho-Stat5 (Tyr694) antibody (no. 4322S, Cell Signaling Technology), Src (no. 2108S, Cell Signaling Technology), Lck (no. 2752S, Cell Signaling Technology), PDGFR $\beta$  (no. 3162S, Cell Signaling Technology). The Millipore immobilon Western chemiluminescence substrate was used for signal development. Blots were imaged in an Amersham Imager 600 (GE Healthcare).

#### 4.2.4. Pharmacokinetic studies

The pharmacokinetic properties of compounds in rats were determined as follows. The compound was administered intravenously to the femoral vein of female Wistar rats as a solution in NMP/PEG200 (1:9, v/v) at 2 mg/kg. Serial plasma samples were collected by sublingual vein bleeding for 24 h (0.083, 0.25, 0.5, 1, 2, 4, 6, 8, 12, 24 h) from one group of rats (n = 3). Samples were extracted and the concentration of compound was determined by LC-MS/MS. LOQ was set to 2.5 ng/mL.

#### 4.2.5. Establishment and analysis of K562 xenograft models

The K562 cell line was stably infected with the lentiviral vector pLVX-IRES-ZsGreen1 carrying the firefly luciferase cDNA and termed K562-Luc cells. Each mouse was inoculated with approximately 200  $\mu$ L of K562-Luc cell suspension ( $2 \times 10^6$  cells) contained 50% Matrigel subcutaneously on the right subventral of NOD/SCID mice. Treatments were initiated when the mean tumor volumes were approximately 200 mm<sup>3</sup>. The compound **17** was formulated in DMSO/PEG 400/40% hydroxypropyl- $\beta$ -cyclodextrin (HP- $\beta$ -CD) (1:3:6, vol/vol) and applied daily by the intraperitoneal administration to the tumor-bearing mice for 10 consecutive days at doses of 1, 3, and 10 mg/kg/qd. Animals were weighed 2–3 times per week during the treatment period. Tumor size was measured utilizing electronic calipers 2–3 times per week during the treatment period. Tumor volume was calculated as  $V = L \times W^2/2$ , where L is the length and W is the width of the tumor. After 10 days, tumor growth measurements were done by noninvasive imaging using a Xenogen IVIS imaging system. Measurements were performed 10 min after intravenous injection of 150 mg/kg (15 mg/mL in PBS) D-luciferin. Mice were euthanized when tumors grew to larger than 2000 mm<sup>3</sup>. All animal experiments were conducted according to the guidelines of the humane use and care of laboratory animals and were approved by the ShanghaiTech University Animal Study Committee (Approval number: 20201026001).

### Declaration of competing interest

The authors declare that they have no known competing financial interests or personal relationships that could have appeared to influence the work reported in this paper.

### Acknowledgement

We are grateful to the Discovery Technology Platform and Analytical platform of Shanghai Institute for Advanced Immunochemical Studies, ShanghaiTech University for technical assistance with LC-MS, MS2, compound screen and flow cytometry experiments. We appreciate the staff members of the National Facility for Protein Science in Shanghai (NFPS), Zhangjiang Lab, China, for providing technical support and assistance in animal handling, data collection and analysis.

This work was supported, in part, by grants from the National Natural Science Foundation of China (NSFC; Grant number 81702600), grants sponsored by Shanghai Sailing Program (Grant number 17YF1412200), and grants sponsored by Shanghai Natural Science Foundation (Grant number 19ZR1433600).

### Appendix A. Supplementary data

Supplementary data to this article can be found online at <https://doi.org/10.1016/j.ejmech.2021.113645>.

### References

- [1] A.C. Lai, C.M. Crews, Induced protein degradation: an emerging drug discovery paradigm, *Nat. Rev. Drug Discov.* 16 (2017) 101–114.
- [2] M. Schapira, M.F. Calabrese, A.N. Bullock, C.M. Crews, Targeted protein degradation: expanding the toolbox, *Nat. Rev. Drug Discov.* 18 (2019) 949–963.
- [3] K.M. Sakamoto, K.B. Kim, A. Kumagai, F. Mercurio, C.M. Crews, R.J. Deshaies, Protacs: chimeric molecules that target proteins to the Skp1-Cullin-F box complex for ubiquitination and degradation, *Proc. Natl. Acad. Sci. U. S. A.* 98 (2001) 8554–8559.
- [4] K.M. Sakamoto, K.B. Kim, R. Verma, A. Ransick, B. Stein, C.M. Crews, R.J. Deshaies, Development of Protacs to target cancer-promoting proteins for ubiquitination and degradation, *Mol. Cell. Proteomics* 2 (2003) 1350–1358.
- [5] G.M. Burslem, B.E. Smith, A.C. Lai, S. Jaime-Figueroa, D.C. McQuaid, D.P. Bondeson, M. Toure, H. Dong, Y. Qian, J. Wang, A.P. Crew, J. Hines, C.M. Crews, The advantages of targeted protein degradation over inhibition: an RTK case study, *Cell Chem. Biol.* 25 (2018) 67–77, e63.
- [6] Y. Zou, D. Ma, Y. Wang, The PROTAC technology in drug development, *Cell Biochem. Funct.* 37 (2019) 21–30.
- [7] J. Peh, M.W. Boudreau, H.M. Smith, P.J. Hergenrother, Overcoming resistance to targeted anticancer therapies through small-molecule-mediated MEK degradation, *Cell Chem. Biol.* 25 (2018) 996–1005 e4.
- [8] Y. Sun, N. Ding, Y. Song, Z. Yang, W. Liu, J. Zhu, Y. Rao, Degradation of Bruton's tyrosine kinase mutants by PROTACs for potential treatment of ibrutinib-resistant non-Hodgkin lymphomas, *Leukemia* 33 (2019) 2105–2110.
- [9] S. Rana, M. Bendjennat, S. Kour, H.M. King, S. Kizhake, M. Zahid, A. Natarajan, Selective degradation of CDK6 by a palbociclib based PROTAC, *Bioorg. Med. Chem. Lett.* 29 (2019) 1375–1379.
- [10] D.P. Bondeson, B.E. Smith, G.M. Burslem, A.D. Buhimschi, J. Hines, S. Jaime-Figueroa, J. Wang, B.D. Hamman, A. Ishchenko, C.M. Crews, Lessons in PROTAC design from selective degradation with a promiscuous warhead, *Cell Chem. Biol.* 25 (2018) 78–87 e75.
- [11] R.B. Kargbo, PROTAC-mediated degradation of KRAS protein for anticancer therapeutics, *ACS Med. Chem. Lett.* 11 (2020) 5–6.
- [12] L. Bai, H. Zhou, R. Xu, Y. Zhao, K. Chinnaswamy, D. McEachern, J. Chen, C.Y. Yang, Z. Liu, M. Wang, L. Liu, H. Jiang, B. Wen, P. Kumar, J.L. Meagher, D. Sun, J.A. Stuckey, S. Wang, A potent and selective small-molecule degrader of STAT3 achieves complete tumor regression in vivo, *Canc. Cell* 36 (2019) 498–511, e417.
- [13] L.H. Jones, Small-molecule kinase downregulators, *Cell Chem. Biol.* 25 (2018) 30–35.
- [14] Y. Wang, X. Jiang, F. Feng, W. Liu, H. Sun, Degradation of proteins by PROTACs and other strategies, *Acta Pharm. Sin. B* 10 (2020) 207–238.
- [15] T. Neklesa, L.B. Snyder, R.R. Willard, N. Vitale, J. Pizzano, D.A. Gordon, et al., ARV-110: an oral androgen receptor PROTAC degrader for prostate cancer, *J. Clin. Oncol.* 37 (2019).
- [16] S. Yamshon, J. Ruan, IMiDs new and old, *Curr. Hematol. Malig. Rep.* 14 (2019) 414–425.

- [17] T. Ito, H. Ando, T. Suzuki, T. Ogura, K. Hotta, Y. Imamura, Y. Yamaguchi, H. Handa, Identification of a primary target of thalidomide teratogenicity, *Science* 327 (2010) 1345–1350.
- [18] T. Ishida, A. Ciulli, E3 ligase ligands for PROTACs: how they were found and how to discover new ones, *SLAS Discov.* 26 (2020) 484–502.
- [19] A.C. Lai, M. Toure, D. Hellerschmied, J. Salami, S. Jaime-Figueroa, E. Ko, J. Hines, C.M. Crews, Modular PROTAC design for the degradation of oncogenic BCR-ABL, *Angew Chem. Int. Ed. Engl.* 55 (2016) 807–810.
- [20] J.D. Rowley, Letter, A new consistent chromosomal abnormality in chronic myelogenous leukaemia identified by quinacrine fluorescence and Giemsa staining, *Nature* 243 (1973) 290–293.
- [21] R. Ren, Mechanisms of BCR-ABL in the pathogenesis of chronic myelogenous leukaemia, *Nat. Rev. Canc.* 5 (2005) 172–183.
- [22] F. Rossari, F. Minutolo, E. Orciuolo, Past, present, and future of Bcr-Abl inhibitors: from chemical development to clinical efficacy, *J. Hematol. Oncol.* 11 (2018), 84.
- [23] C.V. Ichim, Kinase-independent mechanisms of resistance of leukemia stem cells to tyrosine kinase inhibitors, *Stem Cells Transl. Med.* 3 (2014) 405–415.
- [24] A. Hamilton, G.V. Helgason, M. Schemionek, B. Zhang, S. Myssina, E.K. Allan, F.E. Nicolini, C. Muller-Tidow, R. Bhatia, V.G. Brunton, S. Koschmieder, T.L. Holyoake, Chronic myeloid leukemia stem cells are not dependent on Bcr-Abl kinase activity for their survival, *Blood* 119 (2012) 1501–1510.
- [25] F. Lee, A. Fandi, M. Voi, Overcoming kinase resistance in chronic myeloid leukemia, *Int. J. Biochem. Cell Biol.* 40 (2008) 334–343.
- [26] Y. Ru, Q. Wang, X. Liu, M. Zhang, D. Zhong, M. Ye, Y. Li, H. Han, L. Yao, X. Li, The chimeric ubiquitin ligase SH2-U-box inhibits the growth of imatinib-sensitive and resistant CML by targeting the native and T315I-mutant BCR-ABL, *Sci. Rep.* 6 (2016), 28352.
- [27] G.M. Burslem, A.R. Schultz, D.P. Bondeson, C.A. Eide, S.L. Savage Stevens, B.J. Druker, C.M. Crews, Targeting BCR-ABL1 in chronic myeloid leukemia by PROTAC-mediated targeted protein degradation, *Canc. Res.* 79 (2019) 4744–4753.
- [28] Q. Zhao, C. Ren, L. Liu, J. Chen, Y. Shao, N. Sun, R. Sun, Y. Kong, X. Ding, X. Zhang, Y. Xu, B. Yang, Q. Yin, X. Yang, B. Jiang, Discovery of SIA178 as an effective BCR-ABL degrader by recruiting von hippel-lindau (VHL) E3 ubiquitin ligase, *J. Med. Chem.* 62 (2019) 9281–9298.
- [29] Y. Demizu, N. Shibata, T. Hattori, N. Ohoka, H. Motoi, T. Misawa, T. Shoda, M. Naito, M. Kurihara, Development of BCR-ABL degradation inducers via the conjugation of an imatinib derivative and a cIAP1 ligand, *Bioorg. Med. Chem. Lett* 26 (2016) 4865–4869.
- [30] N. Shibata, K. Shimokawa, K. Nagai, N. Ohoka, T. Hattori, N. Miyamoto, O. Ujikawa, T. Sameshima, H. Nara, N. Cho, M. Naito, Pharmacological difference between degrader and inhibitor against oncogenic BCR-ABL kinase, *Sci. Rep.* 8 (2018), 13549.
- [31] K. Shimokawa, N. Shibata, T. Sameshima, N. Miyamoto, O. Ujikawa, H. Nara, N. Ohoka, T. Hattori, N. Cho, M. Naito, Targeting the allosteric site of oncoprotein BCR-ABL as an alternative strategy for effective target protein degradation, *ACS Med. Chem. Lett.* 8 (2017) 1042–1047.
- [32] N. Shibata, N. Miyamoto, K. Nagai, K. Shimokawa, T. Sameshima, N. Ohoka, T. Hattori, Y. Imaeda, H. Nara, N. Cho, M. Naito, Development of protein degradation inducers of oncogenic BCR-ABL protein by conjugation of ABL kinase inhibitors and IAP ligands, *Canc. Sci.* 108 (2017) 1657–1666.
- [33] Y. Yang, H. Gao, X. Sun, Y. Sun, Y. Qiu, Q. Weng, Y. Rao, Global PROTAC toolbox for degrading BCR-ABL overcomes drug-resistant mutants and adverse effects, *J. Med. Chem.* 63 (2020) 8567–8583.
- [34] B. Tong, J.N. Spradlin, L.F.T. Novaes, E. Zhang, X. Hu, M. Moeller, S.M. Brittain, L.M. McGregor, J.M. McKenna, J.A. Tallarico, M. Schirle, T.J. Maimone, D.K. Nomura, A nimbolide-based kinase degrader preferentially degrades oncogenic BCR-ABL, *ACS Chem. Biol.* 15 (2020) 1788–1794.
- [35] L. Jiang, Y. Wang, Q. Li, Z. Tu, S. Zhu, S. Tu, Z. Zhang, K. Ding, X. Lu, Design, synthesis, and biological evaluation of Bcr-Abl PROTACs to overcome T315I mutation, *Acta Pharm. Sin. B* 11 (2021) 1315–1328.
- [36] P.P. Piccaluga, S. Paolini, G. Martinelli, Tyrosine kinase inhibitors for the treatment of Philadelphia chromosome-positive adult acute lymphoblastic leukemia, *Cancer* 110 (2007) 1178–1186.
- [37] M. Steinberg, Dasatinib: a tyrosine kinase inhibitor for the treatment of chronic myelogenous leukemia and philadelphia chromosome-positive acute lymphoblastic leukemia, *Clin. Therapeut.* 29 (2007) 2289–2308.
- [38] A. Zagidullin, V. Milyukov, A. Rizvanov, E. Bulatov, Novel approaches for the rational design of PROTAC linkers, *Explor. Target Antitumor. Ther.* 1 (2020) 381–390.
- [39] C. Donoghue, M. Cubillos-Rojas, N. Gutierrez-Prat, C. Sanchez-Zarzalejo, X. Verdager, A. Riera, A.R. Nebreda, Optimal linker length for small molecule PROTACs that selectively target p38alpha and p38beta for degradation, *Eur. J. Med. Chem.* 201 (2020), 112451.
- [40] K. Cyrus, M. Wehenkel, E.Y. Choi, H.J. Han, H. Lee, H. Swanson, K.B. Kim, Impact of linker length on the activity of PROTACs, *Mol. Biosyst.* 7 (2011) 359–364.
- [41] N.P. Shah, C. Tran, F.Y. Lee, P. Chen, D. Norris, C.L. Sawyers, Overriding imatinib resistance with a novel ABL kinase inhibitor, *Science* 305 (2004) 399–401.
- [42] J.S. Tokarski, J.A. Newitt, C.Y. Chang, J.D. Cheng, M. Wittekind, S.E. Kiefer, K. Kish, F.Y. Lee, R. Borzilleri, L.J. Lombardo, D. Xie, Y. Zhang, H.E. Klei, The structure of Dasatinib (BMS-354825) bound to activated ABL kinase domain elucidates its inhibitory activity against imatinib-resistant ABL mutants, *Canc. Res.* 66 (2006) 5790–5797.
- [43] J. Cortes, E. Jabbour, H. Kantarjian, C.C. Yin, J. Shan, S. O'Brien, G. Garcia-Manero, F. Giles, M. Breeden, N. Reeves, W.G. Wierda, D. Jones, Dynamics of BCR-ABL kinase domain mutations in chronic myeloid leukemia after sequential treatment with multiple tyrosine kinase inhibitors, *Blood* 110 (2007) 4005–4011.
- [44] N.P. Shah, B.J. Skaggs, S. Branford, T.P. Hughes, J.M. Nicoll, R.L. Paquette, C.L. Sawyers, Sequential ABL kinase inhibitor therapy selects for compound drug-resistant BCR-ABL mutations with altered oncogenic potency, *J. Clin. Invest.* 117 (2007) 2562–2569.